De-novo assembly of zucchini genome reveals a whole genome duplication associated with the origin of the *Cucurbita* genus

Javier Montero-Pau[1#], José Blanca[1#], Aureliano Bombarely[2], Peio Ziarsolo[1], Cristina Esteras[1], Carlos Martí-Gómez[1], María Ferriol[3], Pedro Gómez[4], Manuel Jamilena[5], Lukas Mueller[6], Belén Picó[1*] & Joaquín Cañizares[1*]

[1] Institute for the Conservation and Breeding of Agricultural Biodiversity (COMAV-UPV), Universitat Politècnica de València, Camino de Vera s/n, 46022 Valencia, Spain
[2] Department of Horticulture, Virginia Polytechnic Institute and State University, Blacksburg, VA 24061–0002, USA
[3] Instituto Agroforestal Mediterráneo (IAM), Universitat Politècnica de València, Camino de Vera s/n, 46022 Valencia, Spain
[4] IFAPA Centro La Mojonera, Camino de San Nicolás, 1, 04745 La Mojonera, Almería, Spain
[5] Department of Biology and Geology, Research Centers CIAIMBITAL and CeiA3, University of Almeria, 04120 Almería, Spain
[6] Boyce Thompson Institute for Plant Research, Tower Road. Ithaca, NY 14853, USA

[#] Both authors contributed equally
*Corresponding authors.

Corresponding author email addresses: jcanizares@upv.es, mpicosi@btc.upv.es

Abstract

The *Cucurbita* genus (squashes, pumpkins, gourds) includes important domesticated species such as *C. pepo, C. maxima* and *C. moschata*. In this study, we present a high-quality draft of the zucchini (*C. pepo*) genome. The assembly has a size of 263 Mb, a scaffold N50 of 1.8 Mb, 34,240 gene models, includes 92% of the conserved BUSCO core gene set, and it is estimated to cover 93.0% of the genome. The genome is organized in 20 pseudomolecules, that represent 81.4% of the assembly, and it is integrated with a genetic map of 7,718 SNPs. Despite its small genome size three independent evidences support that the *C. pepo* genome is the result of a Whole Genome Duplication: the topology of the gene family phylogenies, the karyotype organization, and the distribution of 4DTv distances. Additionally, 40 transcriptomes of 12 species of the genus were assembled and analyzed together with all the other published genomes of the Cucurbitaceae family. The duplication was detected in all the *Cucurbita* species analyzed, including *C. maxima* and *C. moschata*, but not in the more distant cucurbits belonging to the *Cucumis* and *Citrullus* genera, and it is likely to have happened 30 ± 4 Mya in the ancestral species that gave rise to the genus.

Introduction

Cucurbita pepo L. is the main crop of the *Cucurbita* genus. At the subspecies rank, three taxa are recognised: subsp. *pepo*, known only in cultivation (zucchini, pumpkins, and summer and winter squashes), subsp. *ovifera* (L.) Decker (= subsp. *texana* (Scheele) Filov), known in cultivation and in the wild (scallop and acorn squashes, ornamental gourds), and subsp. *fraterna* (L. H. Bailey) Lira, Andres & Nee (= *C. fraterna* L. H. Bailey), known only in wild populations[1–3]. Subspecies *pepo* and *ovifera* include many edible-fruited cultivar-groups, such as Pumpkin, Vegetable Marrow, Cocozelle, Zucchini, Acorn, Scallop, Straightneck and Crookneck. There is evidence of an early domestication of this species[4], with more than one domestication event, in Mexico and United States[5], and it has had two different diversification processes; one in America and one in Europe[6], where Zucchini and other elongated forms, such as Vegetable Marrow and Cocozelle, were developed.

Cucurbita pepo is an economically important crop. Its production reached 25 million tonnes in 2014, with nearly two million cultivated hectares (http://www.fao.org/faostat/en). Cultivated varieties display a rich diversity on vine, flowering and fruit traits, and among them, cultivars of the Zucchini group rank among the highest-valued vegetables worldwide[7]. The *Cucurbita* genus and the Cucurbitaceae family contain other important crops, such as other squashes, pumpkins and gourds (*Cucurbita maxima* Duchesne and *Cucurbita moschata* (Duchesne ex Lam.) Duchesne ex Poir.), melon (*Cucumis melo* L.), cucumber (*Cucumis sativus* L.) and watermelon (*Citrullus lanatus* (Thunb.) Mansf).

Despite the agronomic importance of the species, before the genome assembly presented here, only a few *C. pepo* genetic and genomic resources were available: a first generation of genetic maps constructed with AFLP, RAPD and SSR markers[8–12], that were later improved with SNPs[13], and several transcriptomes[14–17]. More recently, a high density SNP based genetic map was developed using a RIL population derived from the cross between two *C. pepo* subspecies (subsp. *pepo* Zucchini × subsp. *ovifera* Scallop)[18]. This map was developed to assist us with the *de-novo* assembly process.

In the current study, we present a *de novo* assembly of the *C. pepo* genome, a high coverage transcriptome of *C. pepo*, and 40 transcriptomes of 12 species of the *Cucurbita* genus. The comparative and phylogenetic analyses show that a Whole Genome Duplication (WGD) happened just before the speciations that created this genus. All these resources and several previous transcriptome and draft genome versions are publicly available at https://bioinf.comav.upv.es/downloads/zucchini

Material and Methods

Plant material, genetic material isolation and NGS sequencing

Genomic DNA was isolated from nuclei of the *Cucurbita pepo* subsp. *pepo* cultivar-group Zucchini, accession BGV004370 (also referred to as MU-CU-16 and held at the COMAV-UPV Genebank, https://www.comav.upv.es). Leaves were frozen in liquid nitrogen, crushed in a mortar, and put in a solution of 0.4 mM sucrose, 10 mM Tris-HCL pH 8.0, 10 mM $MgCl_2$ and 5 mM β-mercaptoethanol (20 ml per gram of leaves). This mixture was incubated on ice for 5 minutes. To eliminate debris and cellular fragments, samples were successively filtered through two filters (140 and a 70 μm respectively), and then centrifuged at 3000 g during 20 minutes at 4 ºC. The pellet was resuspended in a solution of 0.25 mM sucrose, 10 mM Tris-HCl pH 8.0, 10 mM $MgCl_2$, 1% Triton X-100 and 5 mM β-mercaptoethanol (1 ml per gram of leaves), and centrifuged again at 12000 g for 10 minutes at 4 ºC. Finally, the pellet was resuspended in 0.5 ml of 1.7 mM sucrose, 10 mM Tris-HCl ph 8.0, 2 mM $MgCl_2$, 0.15 % triton X-100 and 5 mM β-mercaptoethanol, and then centrifuged at 18000 g during 1 hour at 4 ºC. The precipitated nuclei were resuspended in CTAB buffer and the DNA was extracted using the CTAB protocol[19]. Five genomic libraries were prepared: a 500 bp pair-end library and four mate-pair libraries of 3, 7, 10 and 20 Kb insert size respectively. The first three libraries were prepared and sequenced by Macrogen (Seul, Republic of Korea) using two Illumina Hiseq2000 lanes, one for the pair-end library and another for the 3 and 7 Kb mate-pair libraries. The 10 and 20 Kb libraries were prepared by the Boyce Thompson Institute (Ithaca, New York, USA) using the Nextera protocol and were sequenced in a single Illumina Hiseq 2000 lane.

Two different sets of transcriptomes were obtained in the present study: 1) a multi-tissue transcriptome from two cultivars, representing the two main *C. pepo* subspecies to assist the genome annotation, and 2) a group of 40 transcriptomes from 12 different wild and cultivated species of the *Cucurbita* genus for the phylogenetic and comparative analyses (see Suppl. Table 1). In all cases, RNA was isolated using TRI Reagent (Sigma), treated with DNAse and purified by a chloroform and ethanol precipitation. For the *C. pepo* transcriptome, two cultivars with contrasting phenotypes were used (BGV004370 or MU-CU-16, subsp. *pepo* cultivar-group Zucchini; and BGV005203 or UPV-196, subsp. *ovifera* cultivar-group Scallop). RNA was extracted from different tissues: roots, leaves, apical shoots from plants in the male and female phase of development, flower buds collected at two early stages of flower development, mature flowers, pre-harvest fruits at different days after pollination, and post-harvest fruits subjected to different postharvest treatments (ethylene, methylcyclopropene and cold). Equivalent amounts of RNA from each tissue were mixed into two pools, one per cultivar, and two independent cDNA libraries were prepared and sequenced in an Illumina Hiseq2000 lane by Macrogen (Seul, Republic of Korea).

In the case of the 40 transcriptomes, the analyzed species included, besides the two *C. pepo* cultivars used in the multi-tissue transcriptome (Zucchini and Scallop), five additional genotypes of *C.pepo* (one subsp. *ovifera* (Acorn), two subsp. *pepo* (Pumpkin), and two

subsp. *fraterna*). Also the four additional domesticated taxa within the species were represented: *C. moschata* (three transcriptomes), *C. maxima* (three) and its wild ancestor *C. maxima* subsp. *andreana* Naudin (South America and Africa) (one), *C. argyrosperma* Huber (Southern USA and Central America) (five), and *C. ficifolia* Bouché (Guatemala) (two), as well as six wild species occurring in Mexico and Central and South America: the mesophytic annuals *C. ecuadorensis* Cutler & Whitaker (three), *C. okeechobeensis* (Small) L.H Bailey subsp. *martinezii* (L.H.Bailey) T.C. Andres & G.P. Nabhan ex T.W. Walte (three), and *C. lundelliana* L.H Bailey (four) and the xerophytic perennials *C. foetidissima* Kunth (four), *C. cordata* S.Watson (two) and *C. pedatifolia* L.H.Bailey (three). RNA was extracted exclusively from young leaves and the cDNA libraries were prepared and sequenced in a Hiseq2000 lane in the Boyce Thompson Institute (Ithaca, New York, USA).

De-novo genome assembly

The pair-end and mate-pair reads were cleaned using the *ngs_crumbs* software (code available at https://github.com/JoseBlanca/) to eliminate adapters, low quality bases (Phred quality < 25 in a 5 bp window), reads shorter than 50 bp, and duplicated sequences. The Nextera mate-pair reads (10 Kb and 20 Kb libraries) were classified by NextClip v0.8[20] according to the presence of the junction adaptor. Only the mate-pairs in which NextClip was able to detect and trim the adaptor were used for the assembly. For the pre-Nextera mate-pair libraries, the detection and filtering of possible chimeric pairs was done by mapping the reads against a first assembly of the genome and only the pairs with the expected orientation and at the expected distance were kept. The implementation of this process can be found in the *classify_chimeras* and *trim_mp_chimeras* binaries of the *ngs_chrumbs* software. The mitochondrial and chloroplastic reads were detected by blasting[21] them against the *C. melo* organelle genomes (JF412791.1 and NC014050.1). Mitochondrial and chloroplastic reads were also included in the assembly, but only enough randomly selected reads to get a 150X coverage. Assemblies with k-mer lengths from 31 to 61 with a step-size of 4 were carried out. The final assembly was done by SOAPdenovo2 v2.04[22] using k-mer size of 41. Resulting scaffolds were broken with BreakScaffolds (https://github.com/aubombarely/GenoToolBox) and reassembled with SSPACE[23]. The new scaffolds were improved using SOAPdenovo2's GapCloser[22]. Gene completeness of the assembly was assessed using BUSCO v.2[24]. Mitochondrial and chloroplastic scaffolds were identified using BLAST[21] against the chloroplast and mitochondrial genomes of *C. melo*. Genome size was estimated from the k-mer depth distribution as $\sum(d \cdot k_d) / D$ where d is the k-mer depth, k_d is the number of k-mers for the given depth and D is the maximum k-mer depth of the distribution. The leftmost part of the distribution was discarded as it includes mostly k-mers due to sequencing errors. The k-mer distribution was calculated by Jellyfish[25] using a k-mer size of 31.

In order to detect assembly artifacts and to group scaffolds into pseudomolecules, a genetic map was built. A group of 120 individuals of a F_8 Recombinant Inbreed Line (RIL)[18], developed through single seed descent from a previous Zucchini (BGV004370) x Scallop (BGV005203) F_2[13], were genotyped by Genotyping-by-sequencing (GBS)[26]. SNP calling was performed using Freebayes[27] and a genetic map was constructed using the R packages R/qtl[28] and ASMap[29] (see details in Montero-Pau et al.[18]). Scaffolds that were present in

more than one linkage group in the genetic map were visually explored with Hawkeye[30] and manually splitted. Scaffolds were ordered and oriented according to the genetic map into pseudomolecules.

De-novo transcriptome assembly

Raw reads were processed using *ngs_crumbs* software to eliminate adapter sequences, low quality bases (Phred quality < 25 in a 5 bp window) and sequences shorter than 40 bp. The transcriptome was assembled with the Trinity assembler v2.0.6[31] with default parameters. In the case of the *C. pepo* transcriptome, reads of both cultivars were merged in order to get a more comprehensive representation of the transcriptome. Additionally, reads from a previous 454-based transcriptome[17] were also included. The resulting contigs were reassembled with CAP3[32] to eliminate redundancies. Low complexity transcripts were filtered out using *ngs_crumbs*. Trinity subcomponents were clustered using BLAST into unigene clusters doing a transitive clustering. Any two transcripts that shared an overlap longer than 100 bp and a similarity higher than 97% were considered to belong to the same unigene cluster. Finally, transcripts expressed less than 1 % of the most expressed transcript in each Trinity subcomponent were filtered out using RSEM (http://deweylab.biostat.wisc.edu/rsem/).

Genome annotation

Genome structural annotation was performed using Maker-P[33] (version 2.31.6) with the default parameters. The *C. pepo* transcriptome was used to train Augustus[34] (version 3.0.2) with the default parameters. SNAP[35] (version 2006-07-28) was also trained with the same dataset following the instructions from the Maker-P manual. Repetitive sequences were extracted from the genome reference using RepeatModeler[36] (version 1.0.8). The *C. pepo* transcriptome, repetitive sequences, and training ab-initio gene predictor files were used for the annotation with Maker-P. Functional annotation was performed by sequence homology search using BlastP (minimum E-value of 10^{-10}) with GenBank, TAIR10 and SwissProt protein datasets (downloaded 2014-12-21). Additionally, InterProScan[37] was used to annotate protein domains, extending the annotation to Gene Ontology terms associated with these protein domains. Blast2GO[38] was used to do an annotation based on a Blast search against NCBI's nr database. Functional descriptions were processed using AHRD (https://github.com/groupschoof/AHRD) giving a weight of 100, 50 and 30 to SwissProt, TAIR and GenBank annotation respectively.

A structural and homology-based approach, as described in Campbell et al.[33], was used to annotate the repetitive DNA. Briefly, miniature inverted repeat transposable elements (MITE) and long terminal repeat (LTR) retrotransposons were collected using MITE-Hunter[39], LTR-harvest, and LTR-digest[40,41]. A MITE and LTR library was built after excluding false positives, and selecting representative sequences[42]. This library was used to mask genome sequences with RepeatMasker[36], and the resulting sequences were then processed by RepeatModeler in order to look for other repetitive sequences.

Reference sequences of Copia and Gypsy LTR superfamilies of the retrotranscriptase gene were obtained from GyDB[43]. Sequences were manually aligned, and best fitting nucleotide substitution model (based on Bayesian information criterion) and maximum-likelihood tree

for each superfamily were obtained using IQ-TREE[44,45]. Branch support was computed using the bootstrap ultrafast method.

Transcriptome annotation

Transcripts were blasted against Swiss-Prot, UniRef90, and the *Arabidopsis* proteins. Orthologues with cucumber and *Arabidopsis* were detected using a bi-directional BLAST search. The unigenes were associated to GO terms using Blast2GO software[38]. ORFs were predicted in the unigenes with the aid of the ESTScan software[46].

Comparative genomics

Four complete genomes of three related species belonging to the Cucurbitaceae family were included in the study for comparative genomic analyses: *Citrullus lanatus* (genome v. 1)[47], *Cucumis sativus* var. *sativus* (Chinese long) (v. 2)[48], *C. sativus* var. *hardiwickii* (Royle) Gabaer (PI 183967) (v. 1) and *Cucumis melo* (v. 3.5)[49]. The first three are accessible at www.icugi.org and the later at http://melonomics.net. In order to be able to compare among genomes, the repetitive DNA characterization previously described was performed in these four genomes.

Detection of gene duplications were carried out in the gene families created by using OrthoMCL[50,51] and OrthoMCL DB version 5 on the predicted proteomes of the five cucurbit genomes. In those cases in which more than one transcriptional variant was found for the same gene, only the longest variant was used. Differences in the functional role of the duplicated genes were assessed through GO enrichment tests using R package topGO[52], and REVIGO[53] was used to visualize the results. Rate of transversions on 4-fold degenerate synonymous sites (4DTv) was calculated between pairs of orthologs and paralogs using an in-house Python script. Values were corrected for multiple substitutions[54].

The phylogeny (40 transcriptomes and 5 genomes) was reconstructed using a concatenated method and through a joint estimation of both species and gene trees carried out by Phyldog[55]. For the first approach, single copy genes detected using OrthoMCL that were present in all cucurbit genomes were selected, and then the corresponding *C. pepo* transcript was blasted against the 40 *Cucurbita* spp. transcriptomes. Only the blast hits with an E-value higher than 10^{-60} and a match longer than 200 bp were retained. For each gene family, sequence alignments were built using an iterative refinement method implemented in MAFFT[56]. Alignments with less than 30 species were excluded. All resulting gene families were concatenated and the maximum-likelihood tree was inferred using IQ-TREE[44] using a nucleotide substitution model for each gene[45]. For each partition, the best model was selected based on the Bayesian information criterion (BIC). Branch support was obtained by bootstrap using an ultrafast method[57].

For the Phyldog approach sequences were clustered in ortholog groups by blasting all *C. pepo* genes against all 40 *Cucurbita* spp. transcriptomes and the four cucurbit genomes. Blast hits with an identity lower than 70% and shorter than 200 residues were ignored. For each group, three multiple sequence alignments were obtained using Kalign[58], MUSCLE[59]

and MAFFT[56]. Alignment results were combined and evaluated with T-Coffee[60,61] and only alignments with an alignment score higher than 900 were kept. For each alignment a starting tree for Phyldog was inferred using PhyML[62] assuming the best nucleotide substitution model obtained by jModeltest[63]. Phyldog[55] was then used to simultaneously infer species and gene trees and to detect gene duplication events.

Results

De novo genome assembly

The complete genome of *Cucurbita pepo* has been sequenced using a whole genome shotgun sequencing approach. The Zucchini type (*C. pepo* subsp. *pepo*) accession MU-CU-16 was selfed 4 times before sequencing. This accession is characterized by early flowering, bushy growth habit, high production, and uniform cylindrical dark green fruits. This accession was also used as parental in two previous genetic maps[13,18]. One paired-end, with an insert size of 500 bp, and four mate-pair, with sizes of 3, 7, 10 and 20 Kb, libraries were created and sequenced in 5 Illumina Hiseq2000 lanes, resulting in a genome coverage of 254 X for the pair-end library and 54, 46, 65 and 62 X for the 3, 7, 10 and 20 Kb libraries, respectively (Suppl. Table 2). All reads were quality trimmed and filtered. Additionally, about 40% of the 3 and 7 Kb mate-pair reads were found to be chimeric and filtered out by comparing them against a preliminar assembly (see Suppl. Table 2, Suppl. Fig. 1). This chimeric filtering doubled the contig N50 and tripled the scaffold N50 of the final assembly. Finally, 503 M filtered pair-end reads and 185 M mate-pair reads were used in the assembly. The genome was assembled by SOAPdenovo2[22]. A k-mer size of 41 was chosen for the final assembly because it rendered the highest N50 values (Suppl. Fig 2). The SOAPdenovo2 scaffolds were broken and the scaffolding was redone with SSPACE[23] and GapCloser[22]. The final assembly covered 263 Mb in 26,005 scaffolds and 32,754 contigs with a contig N50 of 110 Kb (L50 = 606 contigs) and a scaffold N50 of 1.8 Mb (L50 = 42 scaffolds) (Table 1). Completeness of the *de novo* assembly was assessed with BUSCO using a plant-specific database of 1440 genes. 92.1% of them were found complete (73.1% as single genes and 19.0% as duplicated) and 2.1% were found fragmented. The Illumina RNAseq reads obtained from the MU-CU-16 accession were mapped with HISAT2 with this genome as reference with a 91.9% success rate. The pair-end reads used to build the assembly were mapped against the assembly with a success rate of 99.4%. From the k-mer distribution genome size was estimated to be 283 Mb, thus 93.0% of the genome would be covered by the assembly. Chloroplastic and mitochondrial scaffolds were detected using Blast: 250 scaffolds were identified as mitochondrial and 13 as chloroplastic (Suppl. Table 3).

The genetic map developed with the RIL population of Zucchini x Scallop (accessions MU-CU-16 x UPV-196)[18] was used to detect chimeric scaffolds and to anchor and order the scaffolds into pseudomolecules. 7,718 SNPs (average of 386 markers/linkage group) were located in the map. Based on the relationship of physical and genetic distances and on the presence of the same scaffold in more than one linkage group, 22 out of the 26,005 scaffolds were identified as chimeric. Those scaffolds were visually inspected and splitted. In

a first attempt, a total of 181 scaffolds could be anchored to 21 pseudomolecules, which represents the 81,4% of the assembled genome. Finally, after the integration of this genetic map with the genetic maps developed by Esteras et al.[13], that was based on data from the F_2 of the same cross, and the genetic map of Holdsworth et al.[64], all scaffolds were grouped into 20 pseudomolecules (Table 2 and Suppl. Table 4). Between 4 and 19 scaffolds were anchored to each pseudochromosome with a length between 8.1 Mb and 21.3 Mb (Table 2). Out of the remaining 25,344 scaffolds, 3,295 were longer than 1Kb and 365 were longer than 20Kb. The average correlation between physical distance and genetic distance was 0.98 (0.94-1.00) (Suppl. Fig. 3). This assembly constitutes genome version 4.1. Some other previous versions were made available to the *Cucurbita* community, but none were published.

Transcriptome and genome annotation

Two cDNA libraries were created for the parent accessions of the RIL population using pooled RNA from different vegetative and reproductive tissues. More than 228 millions of reads were added to the previously available 454-based transcriptome[17]. They were used to create a new transcriptome assembly (version 3.0, available at https://bioinf.comav.upv.es/downloads/zucchini) and to annotate the genome. The transcriptome assembly identified 108,062 transcripts, 65,990 of which included an ORF. GO terms could be assigned to 71.5% of the coding transcripts.

The genome annotation resulted in 34,240 predicted gene models, out of which 27,870 were protein-coding genes (Table 3). These results are similar to those found in melon and cucumber[48,49]. The average gene size was 3,450 bp with an average number of exons of 5.4 (Suppl. Fig. 4). The gene models cover 118 Mb, and their coding regions 35 Mb, which represents 45.3% and 13.7% of assembled genome respectively, and indicates a high degree of genome compaction (Fig. 1A). GO terms could be assigned to 19,784 protein-coding genes out of 27,870 (71,0%) (Suppl. Fig. 5 and Suppl. Fig. 6). Functional descriptions were added to 76.6% of transcripts using AHRD, and 79.2% were tagged with an IntrePro protein domain.

Repetitive elements

We identified that 93 Mb (37.8% of the assembly) consisted of repetitive elements (REs) (Suppl. Fig. 7 and Suppl. Table 5). Long terminal repeats (LTR) represented 50.7% of the identified REs. *Gypsy* and *Copia* were the most abundant LTR superfamilies (24.2% and 19.8% of identified REs, and 3.3% and 2.7% of the total genome). The *Gypsy* LTR abundance is similar to that found in *C. melo, C. lanatus* and *C. sativus,* which ranged from 19.5 to 34.4%, whereas the *Copia* family was less represented than in other Cucurbitaceae genomes (30.9 - 34.4%). Other two LTR superfamilies were more copious in the *C. pepo* genome than in the other cucurbits: *Cassandra* (3% of identified RE vs. 0.1 - 0.8%), and *Caulimovirus* (2.1% vs. 0.26- 0.9%). Satellites and simple repeats constituted 25.2% of all identified REs, which is a larger fraction than in related Cucurbitaceae species (4.4% - 12.4%). *Copia* and *Gypsy* REs were assigned to their different families by building two phylogenetic trees (one for *Copia* and one for *Gypsy*) (Suppl. Fig. 7). All *Copia* and *Gypsy*

families previously identified in *C. melo, C. lanatus* and *C. sativus* were also present in *C. pepo,* except for *Copia/Bianca* and *Gypsy/Ogre* families. In these trees the Gypsy/*Galadriel* and *Copia/Tork4* families were overrepresented in *C. pepo*, so they seem to have suffered a diversification process in this species. Finally, approximately, 24% of REs were not assigned to any class of repetitive or transposable elements (TE).

Comparative genomics

Genes, represented by its longest protein, of the four cucurbit crops: *Cucurbita pepo*, *Cucumis melo, Citrullus lanatus*, and two *Cucumis sativus* cultivars (var. *sativus,* Chinese long; and var. *hardiwickii,* PI 183967) were grouped into gene families using OrthoMCL. The percentage of genes that could be assigned to a gene family in these species ranged from 91.2 to 72.8% (Suppl. Table 6). In *C. pepo* the number of gene families with two or more paralogs was higher than in the other crops (Fig. 2 A). Most *C. pepo* gene families were also present in the other cucurbits (Fig. 2 B), however many of them had more than one gene in *C. pepo* (Fig. 2 C). Most of the Zucchini paralogs were organized in large syntenic regions that cover most of the genome (Fig. 1). Synteny with the other cucurbit species showed that despite some conserved synteny, an extensive chromosomal rearrangements has occurred (Fig. 1). The high number of paralogous genes detected and their synteny suggests that *C. pepo* could have suffered a WGD (Suppl. Tables 7, 8 and 9).

The rate of transversions on 4-fold degenerate synonymous sites (4DTv) is a neutral genetic distance that can be used to estimate relative timing of evolutionary events. The distribution of 4DTvs among paralog pairs for all species, but *C. pepo*, showed a wide peak that ranged from 0.4 to 1.1 with a maximum about 0.6 (Fig. 2 D), whereas for *C. pepo* a more recent and narrower peak centered around 0.12 was found. Speciation can also be relatively dated by computing the 4DTvs between orthologous genes of any pair of species. This showed that the speciation event that gave rise to the *Cucurbita* genus, represented by the pairwise 4DTv distributions of *C. pepo* against *C. lanatus, C. sativus,* and *C. melo,* occurred almost simultaneously with the duplication event found in *C. pepo* (Fig. 2 D).

A total of 40 transcriptomes were assembled by Trinity from Illumina reads for 12 species, this resulted in 18,446 to 67,366 genes and 18,902 to 92,522 transcripts (Suppl Table 1). The species and gene family trees were reconstructed using Phyldog, including both the genomes and these 40 transcriptomes. Phyldog marked the duplication events in the gene family trees and calculated the number of duplications per branch in the species tree. According to Phyldog most gene families suffered a duplication event (90%) in the branch that originated the *Cucurbita* genus (Fig. 3). Additionally, a maximum likelihood phylogeny was reconstructed using a concatenated alignment using IQ-TREE. The topologies recovered by both methods are highly congruent, the species trees based on genomic data, showed that xerophytic perennial species (*C. cordata*, *C. pedatifolia*, and *C. foetidissima*) were in a basal position, while mesophytic annuals or short-lived perennials species of the genus were derived from them and formed a monophyletic taxon. The only remarkable difference between both methods was the position of *C. ficifolia,* IQ-TREE grouped it with the mesophytic species, whereas the Phyldog tree grouped it with the xerophytic species. There are some other minor differences related with the position of some accessions within a

particular species between both trees. Some of these differences are related to suspected hybrid accessions like PI540737 (between *C. pedatifolia* and *C. foetidissima*) or PI532392 (between *C. scabridifolia* and *C.foetidissima*). In general, all nodes are supported by bootstrap values close to 100 except those related with hybrids.

A GO enrichment analysis was carried out on three sets of genes: 1) single copy *C. pepo* genes, 2) all duplicated *C. pepo* genes, and 3) duplicated *C. pepo* genes found to be single copy in the rest of cucurbits (i.e., melon, watermelon and cucumber). Single copy genes were enriched in nucleic acid metabolic processes, DNA repair, DNA replication, DNA recombination, rRNA and tRNA processing, lipid metabolism and embryo development (Suppl. Table 10 and Suppl. Fig. 8). In the gene set found to be duplicated in all species, the most significantly enriched GO terms were: transcription and translation regulation, protein metabolism, transmembrane transport, ribosome biogenesis and signal transduction. The terms enriched in the *C. pepo* exclusive duplication were: NAD biosynthesis, regulation of signal transduction, mitochondrial respiratory chain, regulation of cell cycle and cell structure, intracellular protein transport, pollen and vegetative development, photosynthesis light harvesting, and photoperiodism flowering. Interestingly, other genes related to flower development were also found among the exclusively duplicated genes in *C. pepo* such as EARLY FLOWERING 4, Zinc finger CONSTANS-LIKE 3, flowering locus T, RTF1, CDF73, KNUCKLES, CTR9, flowering locus K, GID1b, FLC EXPRESSOR, FRIGIDA and FPA. Additionally, seven out of 34 genes annotated as “similar to CONSTANS-LIKE protein” were exclusively duplicated in *C. pepo,* as well as five out of 9 genes annotated as “similar to FRIGIDA”.

Discussion

In this study we present the first description of the *C. pepo* genome. This new assembly is organized in 20 pseudomolecules, has a scaffold N50 of 1.8 Mb, and is integrated with a high density genetic map. According to the coverage (92.1%) of the BUSCO conserved gene core set and the percentage of the RNAseq reads (91.1%) and genomic reads (99.4%) mapped against it, the current assembly covers most of the zucchini genome. The genome size inferred by k-mer analysis was 283 Mb, so this assembly would constitute 93.0% of the genome. Thus, this assembly is an almost complete representation of the *C. pepo* genome.

Our results show that *C. pepo* genome has suffered a WGD that took place in the origin of the *Cucurbita* genus. Three independent evidences support this WGD: the topology of the gene family phylogenies, the karyotype organization, and the distribution of 4DTv distances. Phyldog reconstructed the phylogeny of every gene family and by comparing it with the species tree topology inferred where the duplication event likely occurred in each family. According to this analysis most duplications happened in the branch that separated the *Cucurbita* genus from the rest of species in the Cucurbitaceae family. The genome structure shown by the physical location of the pairs of Zucchini paralog genes was characterized by large syntenic regions within this species. These syntenic regions cover most of the genome

and are likely to have been generated by a pseudodiplodization process of an ancestral tetraploid followed by different chromosomal rearrangements. Interestingly, all species of the *Cucurbita* genus (tribe *Cucurbiteae*) present n=20 chromosomes[65,66], whereas species of *Benincaseae* tribe, which include *Cucumis* and *Citrullus* genera, have a different chromosomal organization with n=12 (melon), n=11 (watermelon) or n=7 (cucumber)[66]. A possible poliploidy in the origin of *Cucurbita* was already proposed based on the chromosome number and the number of isoenzyme copies[67,68]. Despite the WGD, the size of the Zucchini genome is similar to that of the other sequenced cucurbits, and also, the number of genes is not much higher. This suggests that most genes were deleted after the WGD event. It might well be the case that there is a selective pressure to keep the genome size of these species within a certain range and that the maintained genes were specifically selected.

The 4DTv distribution found in *C. melo, C. sativus* and *C. lanatus* showed no evidence of a recent WGD[48,49]. These three species present a peak on the 4DTv distribution around (0.6) that corresponds to the ancestral paleohexaploidy (γ) event that happened in the divergence of monocotyledons and dicotyledons (~ 300 Mya)[69]. However, the 4DTv distances between paralog genes within Zucchini showed lower distances characterized by a mode of 0.12. Thus most paralogs seem to have been created by a recent duplication. Additionally, the 4DTv peaks found in the distribution calculated for the orthologous genes between *C. pepo* and melon, cucumber and watermelon can be used to date the Zucchini duplication. These peaks are all very close to the Zucchini duplication peak. Thus, both the 4DTv and gene family phylogenies are consistent with a duplication that happened in the ancestral species that gave rise to the *Cucurbita* genus short after its split from the ancestor of *C. melo*, *C. sativus* and *C. lanatus* about 30 ± 4 My[70]. The evolutionary rate derived from this time estimation is consistent with that found in other plants with a recent WGD like *Nelumbo nucifera* (4DTv = 0.17, 18 Mya)[71], *Glycine max* (0.057, 13 Mya)[72], *Zizania latifolia* (0.07, 13 Mya)[73], and *Setaria italica* (0.38, 70 Mya)[74]. *Populus trichocarpa* would be an exception with a much lower evolution rate (0.1, 60-65 Mya)[75], but this discrepancy could be due to the longer generation time of this plant[76]. This WGD might have provided the *Cucurbita* species a way to generate new gene functions used to adapt to new habitats. In fact, this genus includes both xerophytic species, perennials adapted to dry climates and species adapted to moister or mesophytic environments, either annuals or short-lived perennials, and expands from tropic to template regions of America. For instance, the duplication of the photosynthesis and flower development regulation genes found in the GO enrichment analysis, could have provided mechanisms to adapt flowering to variation in temperature and the duration of days found from Southern USA to Southern South America. Genes of these pathways have been implicated in the adaptation of several crops to different photoperiod and geographical adaptation[77]. FLOWERING LOCUS T has been described as a possible long-distance florigenic signal in the cucurbits[78]. The genus also includes an amazing variation in morphological traits related to vine, fruit and seeds.

In agreement with previous *Cucurbita* phylogenetic studies[79–84], the xerophytic perennial species (*C. cordata*, *C. pedatifolia*, and *C. foetidissima*) were basal to the *Cucurbita* genus. The current analysis supports the relationship among mesophytic species found by Kates et al.[81], and additionally, it clarifies the clustering of the sister species *C. foetidissima* and *C.*

pedatifolia, and *C. lundelliana* and *C. okeechobeensis* that were not previously resolved[81]. The position of *C. ficifolia* remains controversial. The concatenated method clusters it as a basal species to the annual mesophytic taxa, showing a paraphyletic relationship with respect to the perennial taxa, in agreement with Wilson et al. [82] and Kates et al.[81]. However, based on Phyldog, *C. ficifolia* appears as a sister species of *C. pedatifolia* and *C. foetidissima*, in agreement with Zheng et al.[83]. *Cucurbita ficifolia* is a mesophytic species, but shares some morphological features with the xerophytic species. More data is needed to establish the relationship of *C. ficifolia* to the mesophytic/xerophytic species of the genus. Also, this incongruence between trees may be also due to hybridization, as some partially fertile hybrids have been obtained between *C. ficifolia* and *C. lundelliana*, *C. foetidissima* and *C. pedatifolia*[85], or it might be the result of very close speciation events.

This genome assembly constitutes a key resource for the study and breeding of the economically important *C. pepo*. Previous unpublished drafts, made available by us, of this genome have already been used in several publications related to the detection of resistance genes, the study of fruit development or the generation of molecular marker sets[15,64,86]. Additionally, we have assembled 40 transcriptomes for 11 species of the *Cucurbita* genus, which can be a valuable source of molecular markers, as well as the foundation of comparative genomic studies.

Acknowledgements

The authors want to thank the USDA, CATIE, VIR and COMAV-UPV genebanks for providing some of the accessions used in this paper. Authors also thank Cristina Roig, Gorka Perpiña and Eva Maria Martínez for their technical assistance.

Author Contributions Statement

JB, JM-P, BP and JC designed and conceived research**.** JB, PZ, CM and JC contributed to the assembly of the genome and transcriptomes. JM-P, AB and LM realized the annotation of the genome. JM-P integrated genome assembly with genetic maps and analyzed genome duplication studies. BP, CE, MF selected/provided plant materials and maintained all living materials. BP and MF did species classification. JC and CE prepared the DNA samples. JC, CE, MJ and PG participated in the preparation of RNA samples for the libraries. JM-P, JB, BP and JC wrote the manuscript. All authors read and approved the final manuscript.

Additional Information

This work was partially funded by the INIA project RTA2011-00044-C02-2 with contributions of E-RTA2013-00020-C04-03 of the Spanish Instituto Nacional de Investigación y Tecnología Agraria y Alimentaria (INIA) cofunded with FEDER funds (EU), and AGL2014-54598-C2-1-R of the Spanish Ministry of Economy and Competitivity.

Genome assembly and raw sequences are deposited in NCBI under BioProject PRJNA386743. Genome v. 4.1, genome annotation and transcriptome v. 3.0 are also available at http://bioinf.comav.upv.es.

The authors declare that they have no competing financial interests that might have influenced the performance or presentation of the work described in this manuscript.

Tables

Table 1. Assembly statistics of *C. pepo* genome version 4.1.

Table 2. Pseudochromosome summary. Number of scaffolds anchored to each pseudochromosome, total length and length without the 1000 N spacers.

Table 3. Genome annotation summary.

Supplementary Tables

Supplementary Table 1. Accessions of domesticated and wild *Cucurbita* spp. used for transcriptomic and phylogenetic analyses. Number of reads used for assembly the transcriptomes, and number of genes and transcripts obtained are also shown.

Supplementary Table 2. NGS library statistics. Numbers of raw reads, percentage of nucleotides over a 30 quality, coverage, % of reads filtered out during the cleaning process, % of reads without adaptor, % of chimeric reads, number of cleaned reads, coverage of cleaned reads, and percentage of nucleotides over a 30 quality in the clean reads.

Supplementary Table 3. Scaffolds of genome assembly v.3.2. containing chloroplastic and mitochondrial regions. The pseudochromosomes were build out of the version 3.2 scaffolds .

Supplementary Table 4. Genome v.4.1 pseudochromosomes configuration. The order, orientation and size of genome v. 3.2 scaffolds grouped in each pseudochromosomes is shown. Equivalence of pseudochromosomes and linkage groups of Montero-Pau et al. (2016) genetic map is also shown.

Supplementary Table 5. Summary of repetitive elements found in *Cucurbita pepo, Cucumis melo, Cucumis sativus* and *Citrullus lanatus.* All results are expressed in bp.

Supplementary Table 6. Gene family (orthogroups and paralogs in OrthoMCL) identification.

Supplementary Table 7. List of genes that are single copy in *Cucurbita pepo.* Predicted function is also shown.

Supplementary Table 8. List of genes that are duplicated in *Cucurbita pepo.* Predicted function is also shown.

Supplementary Table 9. List of genes that are duplicated in *Cucurbita pepo* but not in *Cucumis melo, Cucumis sativus* or *Citrullus lanatus.* Predicted function is also shown.

Supplementary Table 10. GO term enrichment tests. Results are shown for single copy genes in *Cucurbita pepo,* duplicated genes, and genes that are exclusively duplicated in *C. pepo* when compared with other cucurbit genomes.

Images

Figure 1. Genome organization. A) Circos plot showing paralog gene pairs in *Cucurbita pepo* (red lines). Outer plots represent the proportion of repetitive (blue) or gene coding (green) DNA by 200 Kb windows. B) Genomic synteny between *Cucurbita pepo* and *Cucumis melo, Cucumis sativus* and *Citrullus lanatus.* Lines join single copy orthologs.

Figure 2. Genome duplication. A) Distribution of the number of gene families based on the number of gene copies for *Cucurbita pepo, Cucumis melo, Cucumis sativus* and *Citrullus lanatus*; B) Venn diagram showing the number of gene families, and C) the number of duplicated gene families shared among the cucurbit genomes; D) distribution of the rate of transversions on 4-fold degenerate synonymous sites (4DTv) among paralogs for the five studied genomes. Inset shows the boxplots for the 4DTv distribution between ortholog copies of *C. pepo* and the rest of cucurbit species. Red dashed line shows the duplication event in *C. pepo.*

Figure 3. Phylogeny of *Cucurbita* genus based on a concatenated method (left tree) or a joint estimation of gene and species trees (right tree). Left tree: branch lengths represent genetic distance and only bootstrap values lower than 100 are showed. Right tree: branch length represent proportion of duplicated genes per branch, values shown those proportions of duplicated genes higher than 0.1

Supplementary Images

Supplementary Figure 1. Distribution of sequences of k-mer size 41 for different levels of coverage

Supplementary Figure 2. Distribution of N50 for contigs (A) and scaffolds (B) for different k-mer size values

Supplementary Figure 3. Correlation between genetic and physical distances for each pseudochromosome. Color scale represents fraction of repetitive DNA.

Supplementary Figure 4. Summary of the structural annotation of *C. pepo* genome.

Supplementary Figure 5. Transcriptome GO annotation statistics A) by levels and B) at level 6.

Supplementary Figure 6. Genome GO annotation statistics A) by levels and B) at level 6.

Supplementary Figure 7. Repetitive elements. Fraction of genome covered by different types of repetitive elements in *C. pepo and* four *Cucurbita* genomes (A). Maximum likelihood phylogenetic trees of *C. pepo* elements of *Copia* (B) and *Gypsy* (C) LTR superfamilies based on a fragment of the reverse transcriptase.

Supplementary Figure 8. Results of GO enrichment test. Treemaps for the results of the GO enrichment tests on single copy genes in *Cucurbita pepo,* all duplicated genes in *C. pepo* and genes that are duplicated in *C. pepo* but not in other cucurbit genomes. Area of rectangles represent minus logarithm of enrichment test FDR.

Supplementary data

Supplementary data 1. *Cucurbita pepo* genome assembly 4.1. Fasta file.
Supplementary data 2. *Cucurbita pepo* genome annotation 4.1. GFF file.
Supplementary data 3. *Cucurbita pepo* GO term annotation. Results from Blast2GO.

References

1. Andres, T. C. Cucurbita fraterna, the closest wild relative and progenitor of C. pepo. *Rep. Cucurbit Genet. Coop.* **10,** 69–71 (1987).
2. Decker-Walters, D. S. Evidence for multiple domestication of Cucurbita pepo. *Biology and utilization of the Cucurbitaceae. Cornell University Press, Ithaca NY* 96–101 (1990).
3. Paris, H. S., Doron-Faigenboim, A., Reddy, U. K., Donahoo, R. & Levi, A. Genetic relationships in Cucurbita pepo (pumpkin, squash, gourd) as viewed with high frequency oligonucleotide–targeting active gene (HFO–TAG) markers. *Genet. Resour. Crop Evol.* **62,** 1095–1111 (2015).
4. Smith, B. D. The Initial Domestication of Cucurbita pepo in the Americas 10,000 Years Ago. *Science* **276,** 932–934 (1997).

5. Smith, B. D. Eastern North America as an independent center of plant domestication. *Proc. Natl. Acad. Sci. U. S. A.* **103,** 12223–12228 (2006).
6. Paris, H. S., Lebeda, A., Křistkova, E., Andres, T. C. & Nee, M. H. Parallel Evolution Under Domestication and Phenotypic Differentiation of the Cultivated Subspecies of Cucurbita pepo (Cucurbitaceae). *Econ. Bot.* **66,** 71–90 (2012).
7. Formisano, G. *et al.* Genetic diversity of Spanish Cucurbita pepo landraces: an unexploited resource for summer squash breeding. *Genet. Resour. Crop Evol.* **59,** 1169–1184 (2012).
8. Lee, Y. H., Jeon, H. J., Kim, B. D. & Hong, K. H. Use of random amplified polymorphic DNAs for linkage group analysis in interspecific hybrid F2 generation of Cucurbita. *Journal of The Korean Society for Horticultural Science (Korea Republic)* **36,** (1995).
9. Brown, R. N. & Myers, J. R. A Genetic Map of Squash (Cucurbita sp.) with Randomly Amplified Polymorphic DNA Markers and Morphological Markers. *J. Am. Soc. Hortic. Sci.* **127,** 568–575 (2002).
10. Zraidi, A. *et al.* A consensus map for Cucurbita pepo. *Mol. Breed.* **20,** 375–388 (2007).
11. Zraidi, A., Lelley, T., Lebeda, A., Paris, H. S. & Others. Genetic map for pumpkin Cucurbita pepo using random amplified polymorphic DNA markers. in *Progress in cucurbit genetics and breeding research. Proceedings of Cucurbitaceae 2004, the 8th EUCARPIA Meeting on Cucurbit Genetics and Breeding, Olomouc, Czech Republic, 12-17 July, 2004.* 507–514 (Palack\`y University in Olomouc, 2004).
12. Gong, L., Stift, G., Kofler, R., Pachner, M. & Lelley, T. Microsatellites for the genus Cucurbita and an SSR-based genetic linkage map of Cucurbita pepo L. *Theor. Appl. Genet.* **117,** 37–48 (2008).
13. Esteras, C. *et al.* High-throughput SNP genotyping in Cucurbita pepo for map construction and quantitative trait loci mapping. *BMC Genomics* **13,** 80 (2012).
14. Wyatt, L. E., Strickler, S. R., Mueller, L. A. & Mazourek, M. An acorn squash (Cucurbita

pepo ssp. ovifera) fruit and seed transcriptome as a resource for the study of fruit traits in Cucurbita. *Hortic Res* **2,** 14070 (2015).

15. Xanthopoulou, A. *et al.* De novo transcriptome assembly of two contrasting pumpkin cultivars. *Genom Data* **7,** 200–201 (2016).
16. Vitiello, A. *et al. Unraveling zucchini transcriptome response to aphids*. (PeerJ PrePrints, 2016). doi:10.7287/peerj.preprints.1635v1
17. Blanca, J. *et al.* Transcriptome characterization and high throughput SSRs and SNPs discovery in Cucurbita pepo (Cucurbitaceae). *BMC Genomics* **12,** 104 (2011).
18. Montero-Pau, J. *et al.* An SNP-based saturated genetic map and QTL analysis of fruit-related traits in Zucchini using Genotyping-by-sequencing. *BMC Genomics* **18,** 94 (2017).
19. Doyle, J. J. & Doyle, J. L. Isolation of plant DNA from fresh tissue. *Focus* **12,** 13–15 (1990).
20. Leggett, R. M., Clavijo, B. J., Clissold, L., Clark, M. D. & Caccamo, M. NextClip: an analysis and read preparation tool for Nextera Long Mate Pair libraries. *Bioinformatics* **30,** 566–568 (2014).
21. Altschul, S. F., Gish, W., Miller, W., Myers, E. W. & Lipman, D. J. Basic local alignment search tool. *J. Mol. Biol.* **215,** 403–410 (1990).
22. Luo, R. *et al.* SOAPdenovo2: an empirically improved memory-efficient short-read de novo assembler. *Gigascience* **1,** 18 (2012).
23. Boetzer, M., Henkel, C. V., Jansen, H. J., Butler, D. & Pirovano, W. Scaffolding pre-assembled contigs using SSPACE. *Bioinformatics* **27,** 578–579 (2011).
24. Simão, F. A., Waterhouse, R. M., Ioannidis, P., Kriventseva, E. V. & Zdobnov, E. M. BUSCO: assessing genome assembly and annotation completeness with single-copy orthologs. *Bioinformatics* **31,** 3210–3212 (2015).
25. Marçais, G. & Kingsford, C. A fast, lock-free approach for efficient parallel counting of

occurrences of k-mers. *Bioinformatics* **27,** 764–770 (2011).

26. Elshire, R. J. *et al.* A robust, simple genotyping-by-sequencing (GBS) approach for high diversity species. *PLoS One* **6,** e19379 (2011).
27. Garrison, E. & Marth, G. Haplotype-based variant detection from short-read sequencing. *arXiv [q-bio.GN]* (2012).
28. Broman, K. W., Wu, H., Sen, S. & Churchill, G. A. R/qtl: QTL mapping in experimental crosses. *Bioinformatics* **19,** 889–890 (2003).
29. Taylor, J. D. & Butler, D. ASMap: Linkage map construction using the MSTmap algorithm. *R package version 0. 3--3* (2014).
30. Schatz, M. C., Phillippy, A. M., Shneiderman, B. & Salzberg, S. L. Hawkeye: an interactive visual analytics tool for genome assemblies. *Genome Biol.* **8,** R34 (2007).
31. Grabherr, M. G. *et al.* Full-length transcriptome assembly from RNA-Seq data without a reference genome. *Nat. Biotechnol.* **29,** 644–652 (2011).
32. Huang, X. & Madan, A. CAP3: A DNA sequence assembly program. *Genome Res.* **9,** 868–877 (1999).
33. Campbell, M. S. *et al.* MAKER-P: a tool kit for the rapid creation, management, and quality control of plant genome annotations. *Plant Physiol.* **164,** 513–524 (2014).
34. Hoff, K. J. & Stanke, M. WebAUGUSTUS--a web service for training AUGUSTUS and predicting genes in eukaryotes. *Nucleic Acids Res.* **41,** W123–8 (2013).
35. Korf, I. Gene finding in novel genomes. *BMC Bioinformatics* **5,** 59 (2004).
36. Tempel, S. Using and understanding RepeatMasker. *Methods Mol. Biol.* **859,** 29–51 (2012).
37. Mulder, N. & Apweiler, R. InterPro and InterProScan: tools for protein sequence classification and comparison. *Methods Mol. Biol.* **396,** 59–70 (2007).
38. Conesa, A. & Götz, S. Blast2GO: A Comprehensive Suite for Functional Analysis in Plant Genomics. *Int. J. Plant Genomics* **2008,** 1–12 (2008).

39. Han, Y. & Wessler, S. R. MITE-Hunter: a program for discovering miniature inverted-repeat transposable elements from genomic sequences. *Nucleic Acids Res.* **38,** e199 (2010).

40. Ellinghaus, D., Kurtz, S. & Willhoeft, U. LTRharvest, an efficient and flexible software for de novo detection of LTR retrotransposons. *BMC Bioinformatics* **9,** 18 (2008).

41. Steinbiss, S., Willhoeft, U., Gremme, G. & Kurtz, S. Fine-grained annotation and classification of de novo predicted LTR retrotransposons. *Nucleic Acids Res.* **37,** 7002–7013 (2009).

42. Schnable, P. S. *et al.* The B73 maize genome: complexity, diversity, and dynamics. *Science* **326,** 1112–1115 (2009).

43. Llorens, C. *et al.* The Gypsy Database (GyDB) of mobile genetic elements: release 2.0. *Nucleic Acids Res.* **39,** D70–4 (2011).

44. Nguyen, L.-T., Schmidt, H. A., von Haeseler, A. & Minh, B. Q. IQ-TREE: A Fast and Effective Stochastic Algorithm for Estimating Maximum-Likelihood Phylogenies. *Mol. Biol. Evol.* **32,** 268–274 (2015).

45. Chernomor, O., von Haeseler, A. & Minh, B. Q. Terrace Aware Data Structure for Phylogenomic Inference from Supermatrices. *Syst. Biol.* **65,** 997–1008 (2016).

46. Iseli, C., Jongeneel, C. V. & Bucher, P. ESTScan: a program for detecting, evaluating, and reconstructing potential coding regions in EST sequences. *Proc. Int. Conf. Intell. Syst. Mol. Biol.* 138–148 (1999).

47. Guo, S. *et al.* The draft genome of watermelon (Citrullus lanatus) and resequencing of 20 diverse accessions. *Nat. Genet.* **45,** 51–58 (2012).

48. Huang, S. *et al.* The genome of the cucumber, Cucumis sativus L. *Nat. Genet.* **41,** 1275–1281 (2009).

49. Garcia-Mas, J. *et al.* The genome of melon (Cucumis melo L.). *Proceedings of the National Academy of Sciences* **109,** 11872–11877 (2012).

50. Li, L., Stoeckert, C. J. & Roos, D. S. OrthoMCL: identification of ortholog groups for eukaryotic genomes. *Genome Res.* **13,** 2178–2189 (2003).

51. Fischer, S. *et al.* in *Current Protocols in Bioinformatics* 6.12.1–6.12.19 (John Wiley & Sons, Inc., 2011). doi:10.1002/0471250953.bi0612s35

52. Alexa, A. & Rahnenfuhrer, J. *topGO: Enrichment Analysis for Gene Ontology. R package Version 2.18.0*. (2010).

53. Supek, F., Bošnjak, M., Škunca, N. & Šmuc, T. REVIGO Summarizes and Visualizes Long Lists of Gene Ontology Terms. *PLoS One* **6,** e21800 (2011).

54. Tang, H. *et al.* Unraveling ancient hexaploidy through multiply-aligned angiosperm gene maps. *Genome Res.* **18,** 1944–1954 (2008).

55. Boussau, B. *et al.* Genome-scale coestimation of species and gene trees. *Genome Res.* **23,** 323–330 (2013).

56. Katoh, K., Misawa, K., Kuma, K.-I. & Miyata, T. MAFFT: a novel method for rapid multiple sequence alignment based on fast Fourier transform. *Nucl.Acids Res.* **30,** 3059–3066 (2002).

57. Minh, B. Q., Nguyen, M. A. T. & von Haeseler, A. Ultrafast Approximation for Phylogenetic Bootstrap. *Mol. Biol. Evol.* **30,** 1188–1195 (2013).

58. Lassmann, T., Frings, O. & Sonnhammer, E. L. L. Kalign2: high-performance multiple alignment of protein and nucleotide sequences allowing external features. *Nucleic Acids Res.* **37,** 858–865 (2009).

59. Edgar, R. C. MUSCLE: multiple sequence alignment with high accuracy and high throughput. *Nucleic Acids Res.* **32,** 1792–1797 (2004).

60. Wallace, I. M., O'Sullivan, O., Higgins, D. G. & Notredame, C. M-Coffee: combining multiple sequence alignment methods with T-Coffee. *Nucleic Acids Res.* **34,** 1692–1699 (2006).

61. Chang, J.-M., Di Tommaso, P. & Notredame, C. TCS: a new multiple sequence

alignment reliability measure to estimate alignment accuracy and improve phylogenetic tree reconstruction. *Mol. Biol. Evol.* **31,** 1625–1637 (2014).

62. Guindon, S., Delsuc, F., Dufayard, J.-F. & Gascuel, O. Estimating maximum likelihood phylogenies with PhyML. *Methods Mol. Biol.* **537,** 113–137 (2009).
63. Posada, D. jModeltest: Phylogenetic Model Averaging. *Molecular Biology and Evolution* **25,** 1253–1256 (2008).
64. Holdsworth, W. L., LaPlant, K. E., Bell, D. C., Jahn, M. M. & Mazourek, M. Cultivar-Based Introgression Mapping Reveals Wild Species-Derived Pm-0, the Major Powdery Mildew Resistance Locus in Squash. *PLoS One* **11,** e0167715 (2016).
65. Šiško, M., Ivančič, A. & Bohanec, B. Genome size analysis in the genus Cucurbita and its use for determination of interspecific hybrids obtained using the embryo-rescue technique. *Plant Sci.* **165,** 663–669 (2003/9).
66. Kocyan, A., Zhang, L.-B., Schaefer, H. & Renner, S. S. A multi-locus chloroplast phylogeny for the Cucurbitaceae and its implications for character evolution and classification. *Mol. Phylogenet. Evol.* **44,** 553–577 (2007).
67. Weeden, N. F. Isozyme studies indicate that the genus Cucurbita is an ancient tetraploid. *Rep. Cucurbit Genet. Coop.* (jun1984).
68. Kirkpatrick, K. J., Decker, D. S. & Wilson, H. D. Allozyme differentiation in the Cucurbita pepo complex: C. pepo var. medullosa vs. C. texana. *Econ. Bot.* **39,** 289–299 (1985).
69. Bowers, J. E., Chapman, B. A., Rong, J. & Paterson, A. H. Unravelling angiosperm genome evolution by phylogenetic analysis of chromosomal duplication events. *Nature* **422,** 433–438 (2003).
70. Schaefer, H., Heibl, C. & Renner, S. S. Gourds afloat: a dated phylogeny reveals an Asian origin of the gourd family (Cucurbitaceae) and numerous oversea dispersal events. *Proc. Biol. Sci.* **276,** 843–851 (2009).
71. Wang, Y. *et al.* The sacred lotus genome provides insights into the evolution of

flowering plants. *Plant J.* **76,** 557–567 (2013).

72. Schmutz, J. *et al.* Genome sequence of the palaeopolyploid soybean. *Nature* **463,** 178–183 (2010).
73. Guo, L. *et al.* A host plant genome (Zizania latifolia) after a century-long endophyte infection. *Plant J.* **83,** 600–609 (2015).
74. Zhang, G. *et al.* Genome sequence of foxtail millet (Setaria italica) provides insights into grass evolution and biofuel potential. *Nat. Biotechnol.* **30,** 549–554 (2012).
75. Tuskan, G. A. *et al.* The genome of black cottonwood, Populus trichocarpa (Torr. & Gray). *Science* **313,** 1596–1604 (2006).
76. Smith, S. A. & Donoghue, M. J. Rates of molecular evolution are linked to life history in flowering plants. *Science* **322,** 86–89 (2008).
77. Blümel, M., Dally, N. & Jung, C. Flowering time regulation in crops—what did we learn from Arabidopsis? *Curr. Opin. Biotechnol.* **32,** 121–129 (2015).
78. Lin, M.-K. *et al.* FLOWERING LOCUS T protein may act as the long-distance florigenic signal in the cucurbits. *Plant Cell* **19,** 1488–1506 (2007).
79. Jobst, J., King, K. & Hemleben, V. Molecular evolution of the internal transcribed spacers (ITS1 and ITS2) and phylogenetic relationships among species of the family Cucurbitaceae. *Mol. Phylogenet. Evol.* **9,** 204–219 (1998).
80. Sanjur, O. I., Piperno, D. R., Andres, T. C. & Wessel-Beaver, L. Phylogenetic relationships among domesticated and wild species of Cucurbita (Cucurbitaceae) inferred from a mitochondrial gene: Implications for crop plant evolution and areas of origin. *Proceedings of the National Academy of Sciences* **99,** 535–540 (2002).
81. Kates, H. R., Soltis, P. S. & Soltis, D. E. Evolutionary and domestication history of Cucurbita (pumpkin and squash) species inferred from 44 nuclear loci. *Mol. Phylogenet. Evol.* (2017). doi:10.1016/j.ympev.2017.03.002
82. Wilson, H. D., Doebley, J. & Duvall, M. Chloroplast DNA diversity among wild and

cultivated members of Cucurbita (Cucurbitaceae). *Theor. Appl. Genet.* **84,** 859–865 (1992).

83. Zheng, Y.-H., Alverson, A. J., Wang, Q.-F. & Palmer, J. D. Chloroplast phylogeny of Cucurbita: Evolution of the domesticated and wild species. *Jnl of Sytematics Evolution* **51,** 326–334 (2013).
84. Kistler, L. *et al.* Gourds and squashes (Cucurbita spp.) adapted to megafaunal extinction and ecological anachronism through domestication. *Proc. Natl. Acad. Sci. U. S. A.* **112,** 15107–15112 (2015).
85. Lira-Saade, R. Estudios taxonómicos y ecogeográficos de las Cucurbitaceae Latinoamericanas de importancia económica. Systematic and Ecogeographic Studies on Crop Genepools, No. 9. *Rome: International Plant Genetic Resources Institute* (1995).
86. Martínez, C. *et al.* Involvement of ethylene biosynthesis and signalling in fruit set and early fruit development in zucchini squash (Cucurbita pepo L.). *BMC Plant Biol.* **13,** 139 (2013).

83. Lira-Saade, R. Estudios taxonómicos y ecogeográficos de las Cucurbitaceae Latinoamericanas de importancia económica. Systematic and Ecogeographic Studies on Crop Genepools, No. 9. *Rome: International Plant Genetic Resources Institute* (1995).

Table 1. Assembly statistics of *C. pepo* genome version 4.1

Parameter	**Value**
GC content (%)	36,52
No. of contigs (≥ 0 bp)	32,754
No. of contigs (≥ 500 bp)	13,896
No. of contigs (≥1000 bp)	8,217
Bases in contigs (≥ 0 bp)	247,816,249
Bases in contigs (≥ 1000 bp)	238,245,128
Largest contigs (bp)	639,487
N50 contig size (bp)	110,136
N75 contig size (bp)	49,377
L50 contig number	606
L75 contig number	1,407
No. of scaffolds (≥0 bp)	26.025
No. of scaffolds (≥500 bp)	7,994
No. of scaffolds (≥1000 bp)	3,709
Bases in scaffolds (≥0 bp)	263,500,453
Bases in scaffolds (≥500 bp)	258,108,973
Bases in scaffolds (≥1000 bp)	255,237,628
Largest contig (bp)	6,123,784
N50 scaffold size (bp)	1,749,822
N75 scaffold size (bp)	453,344
L50 scaffold number	42
L75 scaffold number	112

Table 2. Pseudochromosome summary. Number of scaffolds anchored to each pseudochromosome, total length and length without the 1000 N spacers.

Molecule	#Scaffolds	Length (bp)	Length without N spacers (bp)
Cp4.1LG01	19	21,320,769	21,302,769
Cp4.1LG02	16	14,376,414	14,361,414
Cp4.1LG03	12	13,772,414	13,761,414
Cp4.1LG04	5	12,709,140	12,705,140
Cp4.1LG05	8	10,865,678	10,858,678
Cp4.10LG06	11	10,677,745	10,667,745
Cp4.1LG07	14	10,147,556	10,134,556
Cp4.1LG08	4	10,059,303	10,056,303
Cp4.1LG09	10	9,920,322	9,911,322
Cp4.1LG10	8	9,835,092	9,828,092
Cp4.1LG11	11	9,833,969	9,823,969
Cp4.1LG12	5	9,824,194	9,820,194
Cp4.1LG13	8	9,354,089	9,347,089
Cp4.1LG14	5	8,955,933	8,951,933
Cp4.1LG15	4	8,816,444	8,813,444
Cp4.1LG16	10	8,691,934	8,682,934
Cp4.1LG17	9	8,680,504	8,672,504
Cp4.1LG18	7	8,333,454	8,327,454
Cp4.1LG19	8	8,246,682	8,239,682
Cp4.1LG20	7	8,120,804	8,114,804

Table 3. Genome annotation summary

Genes	34,240
Protein coding genes	27,870
mRNAs	27,870
Protein-coding mRNAs	27,870
Exons	184,243
CDSs	166,271
Introns	150,003
5’ UTRs	21,701
3’ UTRs	22,296
tRNAs	6,370

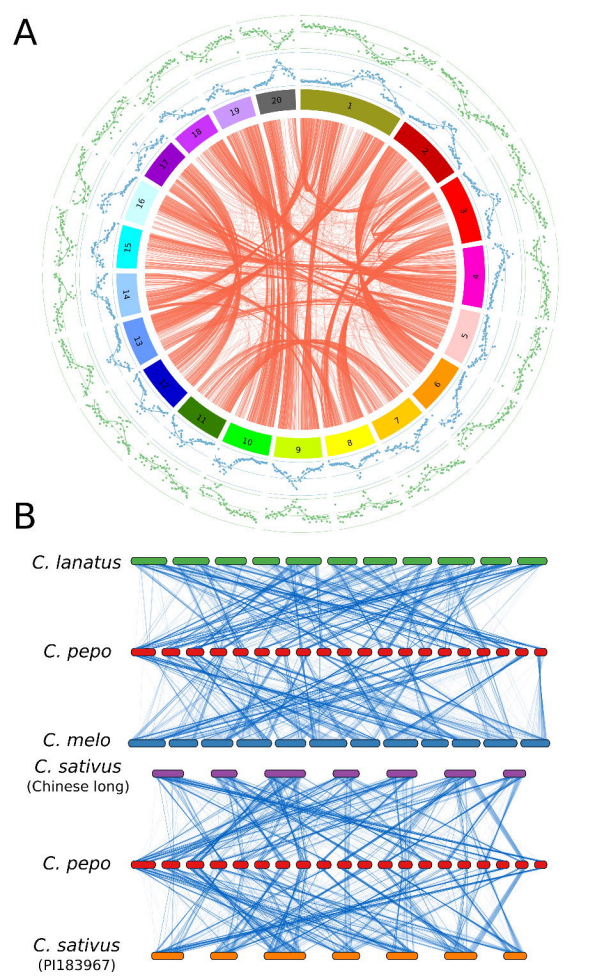
A
20
1
2
3
4
5
6
7
8
9
10
11
12
13
14
15
16
17
18
19
B
C. lanatus
C. pepo
C. melo
C. sativus
(Chinese long)
C. pepo
C. sativus
(PI183967)

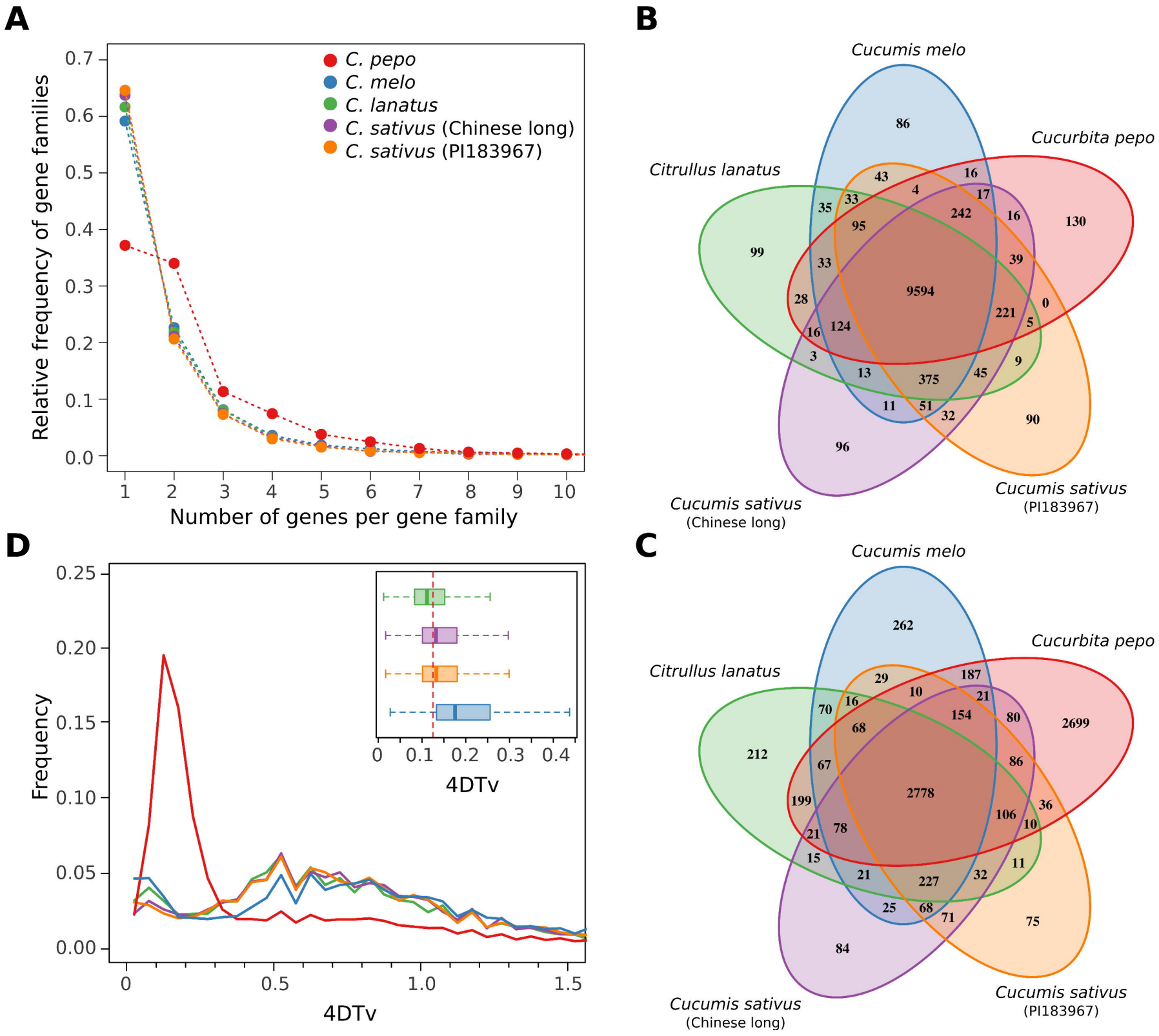
A
Relative frequency of gene families
Number of genes per gene family
C. pepo
C. melo
C. lanatus
C. sativus (Chinese long)
C. sativus (PI183967)
B
Cucumis melo
Cucurbita pepo
Citrullus lanatus
Cucumis sativus (Chinese long)
Cucumis sativus (PI183967)
86
130
99
96
90
9594
2778
262
2699
212
2778
D
Frequency
4DTv
4DTv
C
Cucumis melo
Cucurbita pepo
Citrullus lanatus
Cucumis sativus (Chinese long)
Cucumis sativus (PI183967)

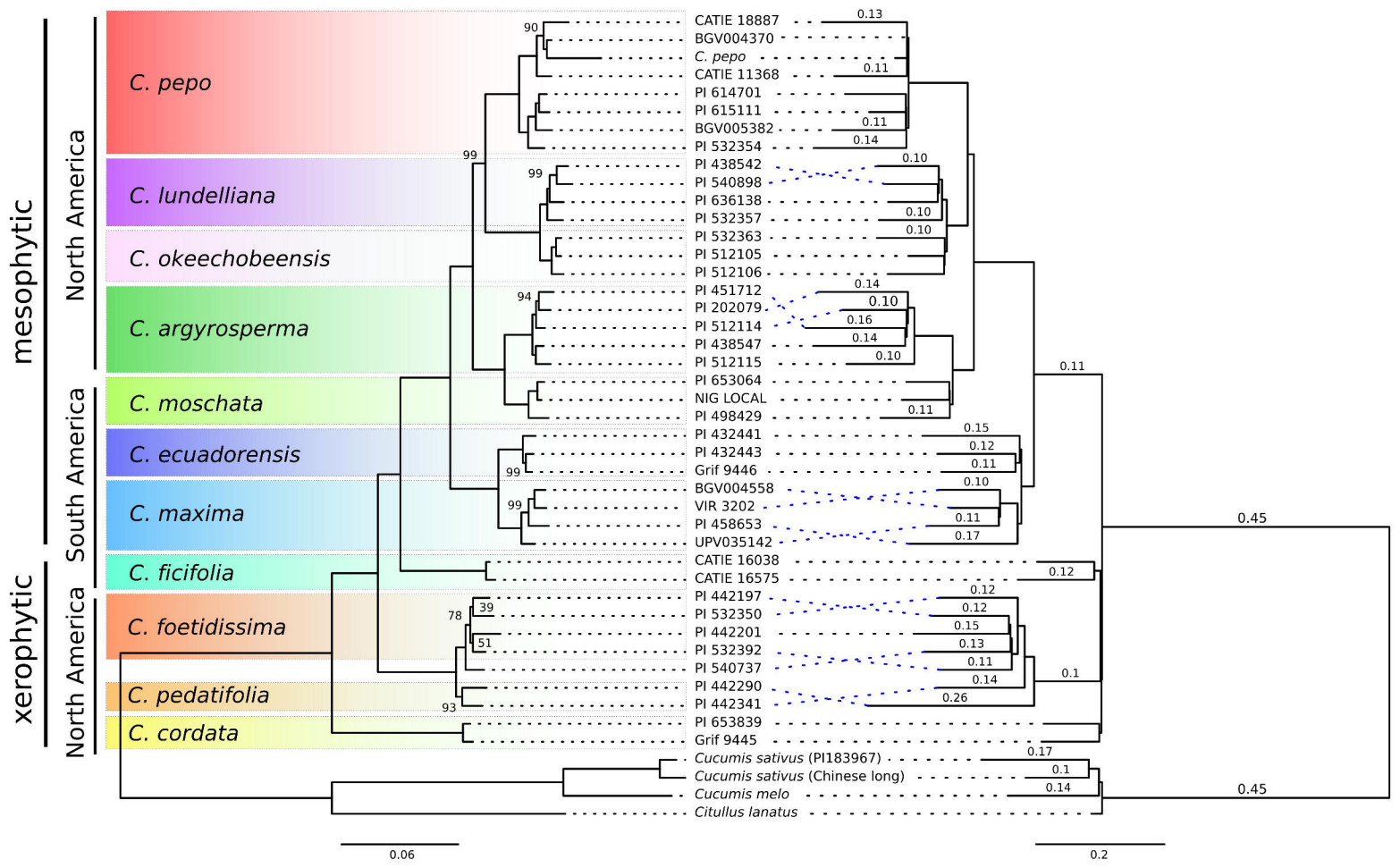
mesophytic
xerophytic
North America
South America
North America
C. pepo
C. lundelliana
C. okeechobeensis
C. argyrosperma
C. moschata
C. ecuadorensis
C. maxima
C. ficifolia
C. foetidissima
C. pedatifolia
C. cordata
CATIE 18887
BGV004370
C. pepo
CATIE 11368
PI 614701
PI 615111
BGV005382
PI 532354
PI 438542
PI 540898
PI 636138
PI 532357
PI 532363
PI 512105
PI 512106
PI 451712
PI 202079
PI 512114
PI 438547
PI 512115
PI 653064
NIG LOCAL
PI 498429
PI 432441
PI 432443
Grif 9446
BGV004558
VIR 3202
PI 458653
UPV035142
CATIE 16038
CATIE 16575
PI 442197
PI 532350
PI 442201
PI 532392
PI 540737
PI 442290
PI 442341
PI 653839
Grif 9445
Cucumis sativus (PI183967)
Cucumis sativus (Chinese long)
Cucumis melo
Citullus lanatus
0.06
0.2

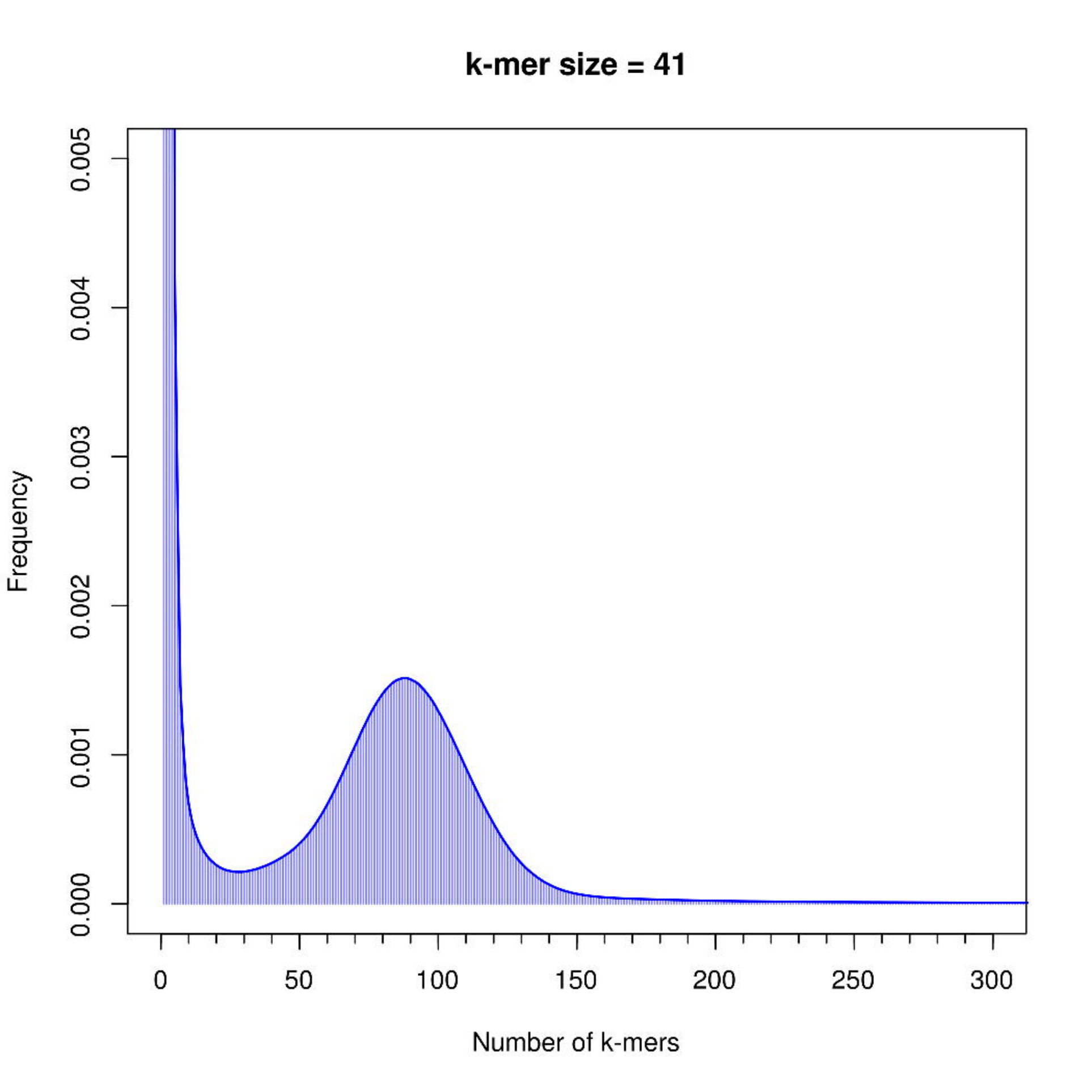
k-mer size = 41
Frequency
0.000
0.001
0.002
0.003
0.004
0.005
0
50
100
150
200
250
300
Number of k-mers

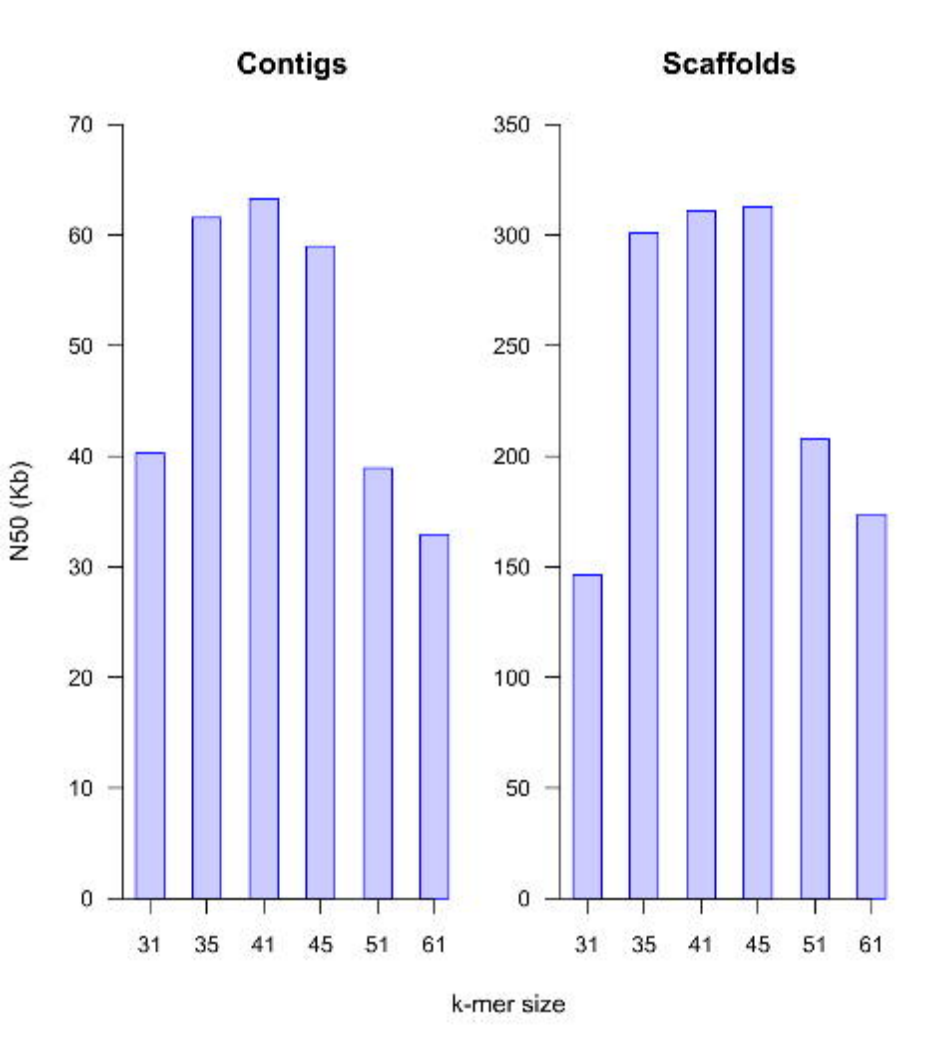
Contigs
Scaffolds
N50 (Kb)
0
10
20
30
40
50
60
70
0
50
100
150
200
250
300
350
31
35
41
45
51
61
k-mer size

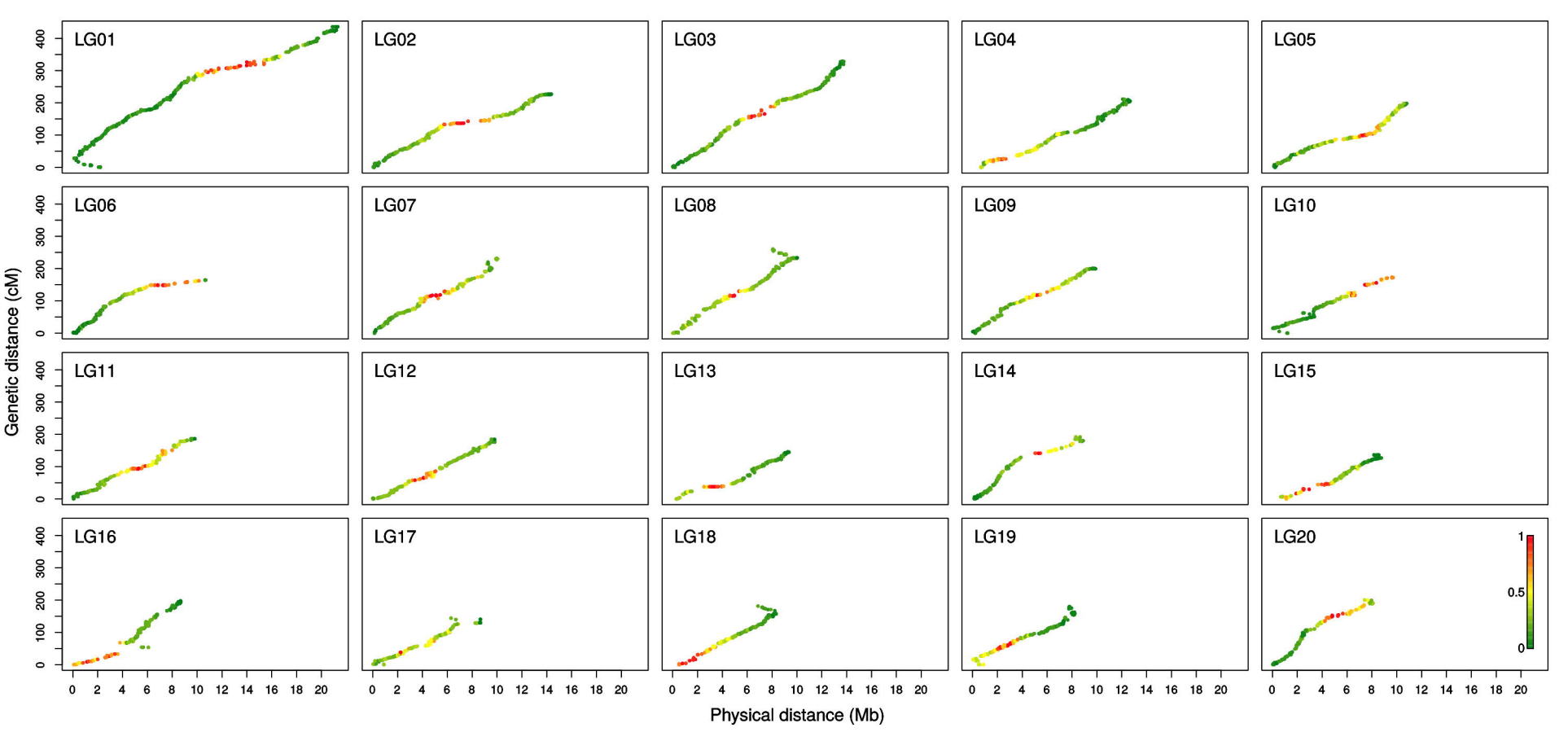
LG01
LG02
LG03
LG04
LG05
LG06
LG07
LG08
LG09
LG10
LG11
LG12
LG13
LG14
LG15
LG16
LG17
LG18
LG19
LG20
Genetic distance (cM)
Physical distance (Mb)
0 100 200 300 400
0 2 4 6 8 10 12 14 16 18 20
1
0.5
0

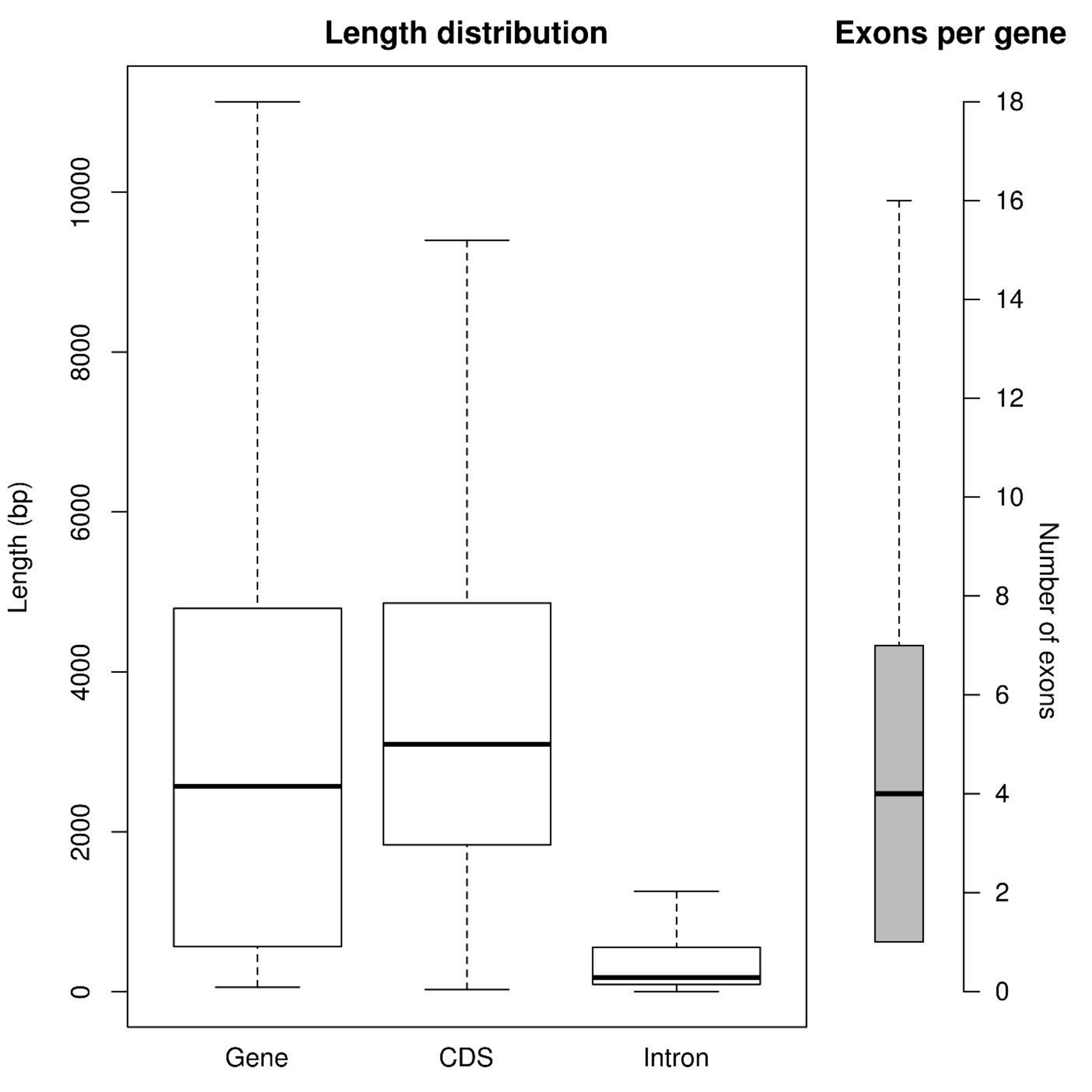
Length distribution
Exons per gene
Length (bp)
0
2000
4000
6000
8000
10000
Gene
CDS
Intron
Number of exons
0
2
4
6
8
10
12
14
16
18

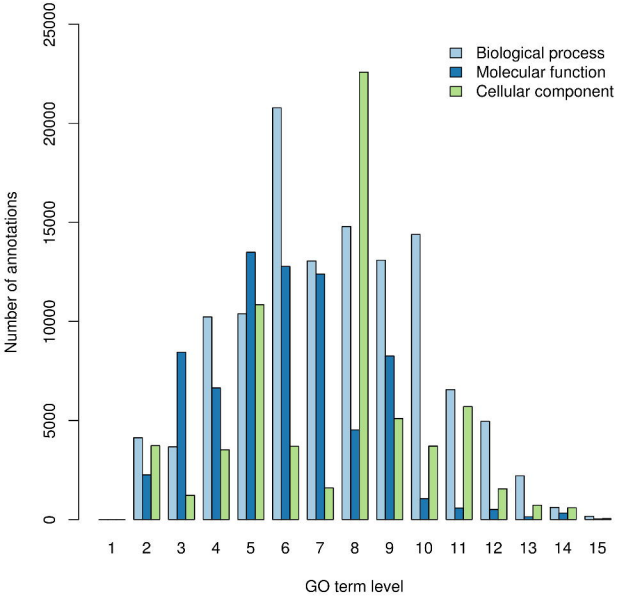
Biological process
Molecular function
Cellular component
Number of annotations
0
5000
10000
15000
20000
25000
1
2
3
4
5
6
7
8
9
10
11
12
13
14
15
GO term level

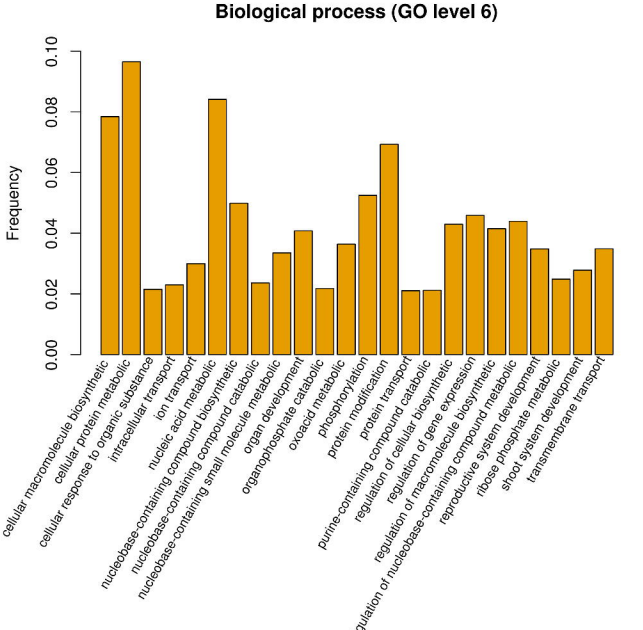
Biological process (GO level 6)
Frequency
0.00
0.02
0.04
0.06
0.08
0.10
cellular macromolecule biosynthetic
cellular protein metabolic
cellular response to organic substance
intracellular transport
ion transport
nucleic acid metabolic
nucleobase-containing compound biosynthetic
nucleobase-containing compound catabolic
nucleobase-containing small molecule metabolic
organ development
organophosphate catabolic
oxoacid metabolic
phosphorylation
protein modification
protein transport
purine-containing compound catabolic
regulation of cellular biosynthetic
regulation of gene expression
regulation of macromolecule biosynthetic
regulation of nucleobase-containing compound metabolic
reproductive system development
ribose phosphate metabolic
shoot system development
transmembrane transport

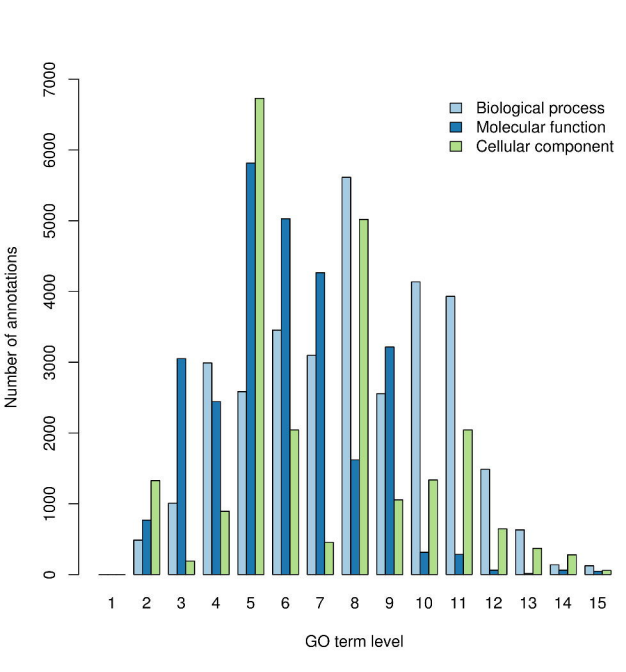
Biological process
Molecular function
Cellular component
Number of annotations
0
1000
2000
3000
4000
5000
6000
7000
1
2
3
4
5
6
7
8
9
10
11
12
13
14
15
GO term level

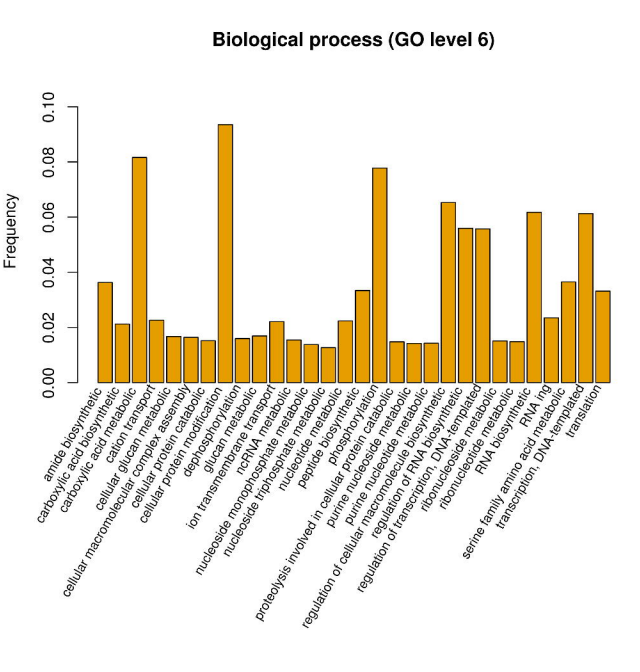
Biological process (GO level 6)
Frequency
0.00
0.02
0.04
0.06
0.08
0.10
amide biosynthetic
carboxylic acid biosynthetic
carboxylic acid metabolic
cation transport
cellular glucan metabolic
cellular macromolecular complex assembly
cellular protein catabolic
cellular protein modification
dephosphorylation
glucan metabolic
ion transmembrane transport
ncRNA metabolic
nucleoside monophosphate metabolic
nucleoside triphosphate metabolic
nucleotide metabolic
peptide biosynthetic
phosphorylation
proteolysis involved in cellular protein catabolic
purine nucleoside metabolic
purine nucleotide metabolic
regulation of cellular macromolecule biosynthetic
regulation of RNA biosynthetic
regulation of transcription, DNA-templated
ribonucleoside metabolic
ribonucleotide metabolic
RNA biosynthetic
RNA ing
serine family amino acid metabolic
transcription, DNA-templated
translation

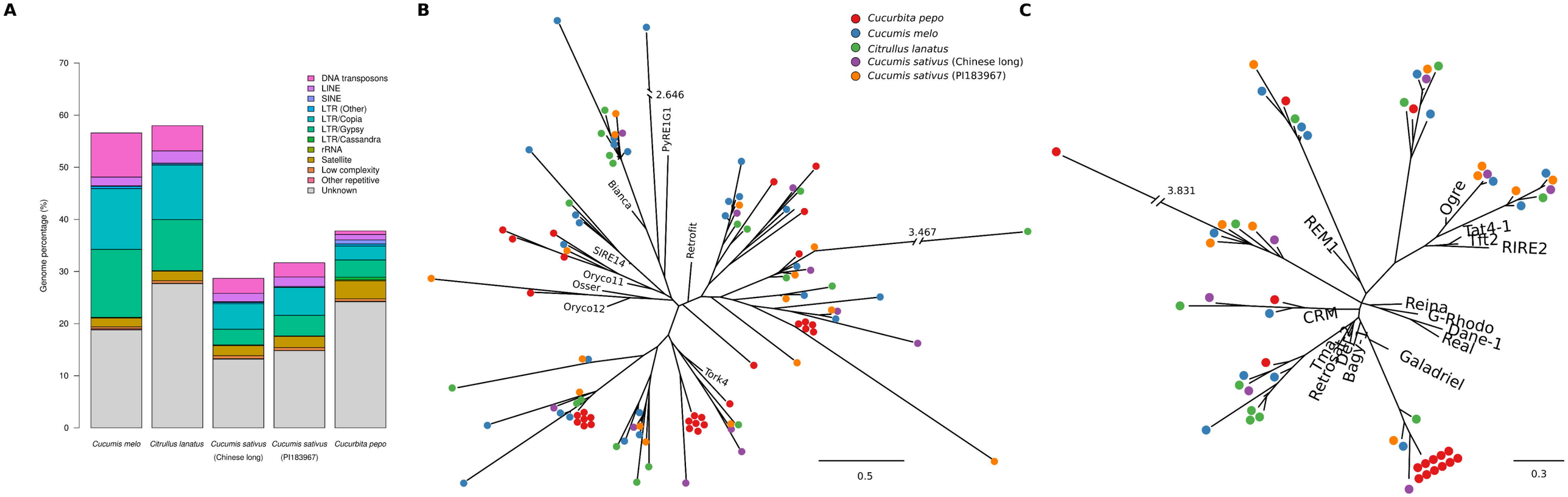
A
Genome percentage (%)
0
10
20
30
40
50
60
70
DNA transposons
LINE
SINE
LTR (Other)
LTR/Copia
LTR/Gypsy
LTR/Cassandra
rRNA
Satellite
Low complexity
Other repetitive
Unknown
Cucumis melo
Citrullus lanatus
Cucumis sativus (Chinese long)
Cucumis sativus (PI183967)
Cucurbita pepo
B
Cucurbita pepo
Cucumis melo
Citrullus lanatus
Cucumis sativus (Chinese long)
Cucumis sativus (PI183967)
2.646
PyRE1G1
Bianca
SIRE14
Oryco11
Osser
Oryco12
Retrofit
3.467
Tork4
0.5
C
3.831
REM1
Ogre
Tat4-1
Ttt2
RIRE2
CRM
Reina
G-Rhodo
Dane-1
Real
Galadriel
Tma
Retrosat2
Del-1
Bagy-1
0.3

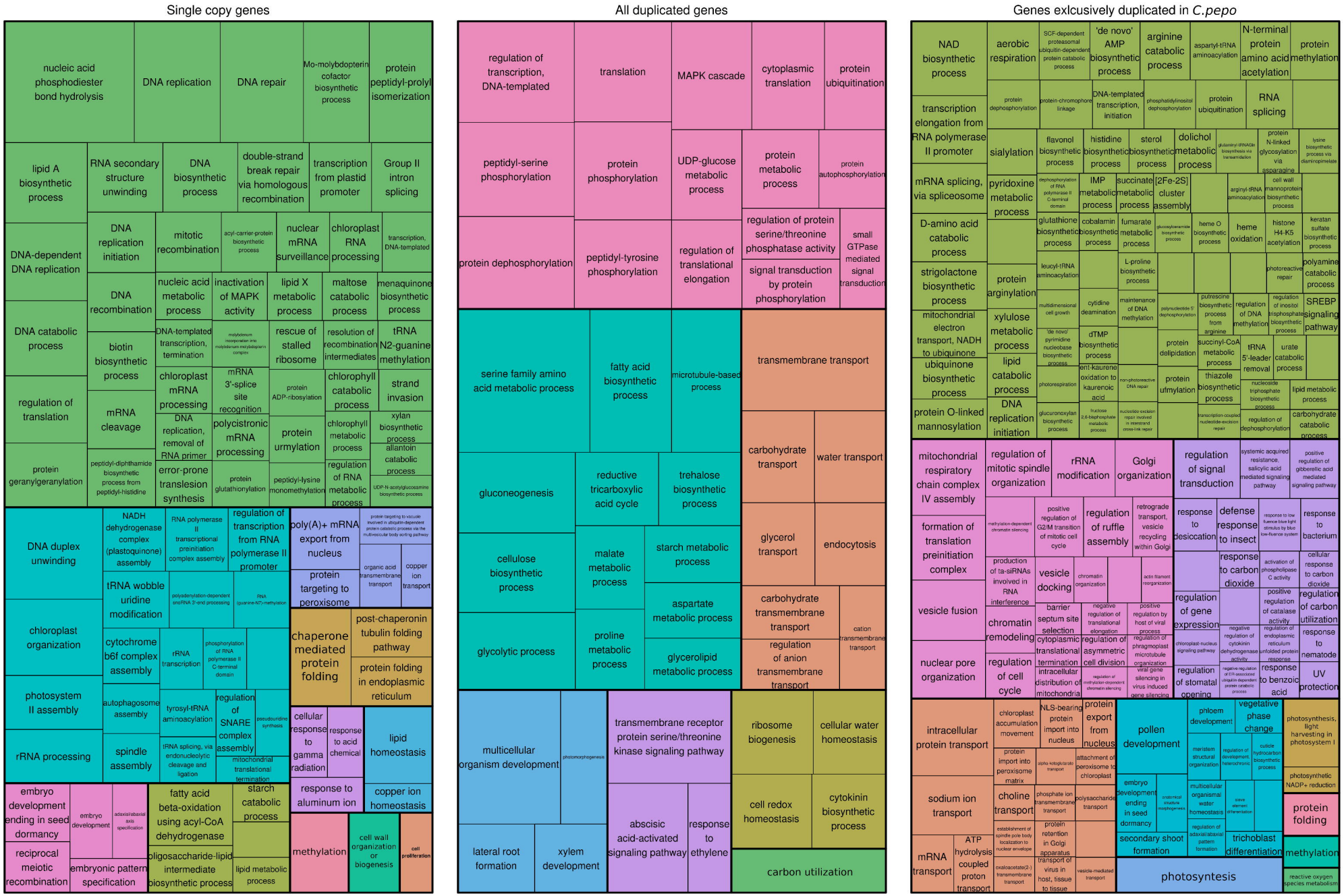
Single copy genes
nucleic acid phosphodiester bond hydrolysis
DNA replication
DNA repair
Mo-molybdopterin cofactor biosynthetic process
protein peptidyl-prolyl isomerization
lipid A biosynthetic process
RNA secondary structure unwinding
DNA biosynthetic process
double-strand break repair via homologous recombination
transcription from plastid promoter
Group II intron splicing
DNA-dependent DNA replication
DNA replication initiation
mitotic recombination
acyl-carrier-protein biosynthetic process
nuclear mRNA surveillance
chloroplast RNA processing
transcription, DNA-templated
DNA recombination
nucleic acid metabolic process
inactivation of MAPK activity
lipid X metabolic process
maltose catabolic process
menaquinone biosynthetic process
DNA catabolic process
DNA-templated transcription, termination
molybdenum incorporation into molybdenum molybdopterin complex
rescue of stalled ribosome
resolution of recombination intermediates
tRNA N2-guanine methylation
biotin biosynthetic process
chloroplast mRNA processing
mRNA 3'-splice site recognition
protein ADP-ribosylation
chlorophyll catabolic process
strand invasion
regulation of translation
mRNA cleavage
DNA replication, removal of RNA primer
polycistronic mRNA processing
protein urmylation
chlorophyll metabolic process
xylan biosynthetic process
protein geranylgeranylation
peptidyl-diphthamide biosynthetic process from peptidyl-histidine
error-prone translesion synthesis
protein glutathionylation
peptidyl-lysine monomethylation
regulation of RNA metabolic process
allantoin catabolic process
UDP-N-acetylglucosamine biosynthetic process
DNA duplex unwinding
NADH dehydrogenase complex (plastoquinone) assembly
RNA polymerase II transcriptional preinitiation complex assembly
regulation of transcription from RNA polymerase II promoter
poly(A)+ mRNA export from nucleus
protein targeting to vacuole involved in ubiquitin-dependent protein catabolic process via the multivesicular body sorting pathway
tRNA wobble uridine modification
polyadenylation-dependent snoRNA 3'-end processing
RNA guanine-N7-methylation
organic acid transmembrane transport
copper ion transport
protein targeting to peroxisome
chloroplast organization
chaperone mediated protein folding
post-chaperonin tubulin folding pathway
cytochrome b6f complex assembly
rRNA transcription
phosphorylation of RNA polymerase II C-terminal domain
protein folding in endoplasmic reticulum
photosystem II assembly
autophagosome assembly
tyrosyl-tRNA aminoacylation
regulation of SNARE complex assembly
pseudouridine synthesis
cellular response to gamma radiation
response to acid chemical
lipid homeostasis
rRNA processing
spindle assembly
tRNA splicing, via endonucleolytic cleavage and ligation
mitochondrial translational termination
response to aluminum ion
copper ion homeostasis
embryo development ending in seed dormancy
embryo development
adaxial/abaxial axis specification
fatty acid beta-oxidation using acyl-CoA dehydrogenase
starch catabolic process
methylation
cell wall organization or biogenesis
cell proliferation
reciprocal meiotic recombination
embryonic pattern specification
oligosaccharide-lipid intermediate biosynthetic process
lipid metabolic process
All duplicated genes
regulation of transcription, DNA-templated
translation
MAPK cascade
cytoplasmic translation
protein ubiquitination
peptidyl-serine phosphorylation
protein phosphorylation
UDP-glucose metabolic process
protein metabolic process
protein autophosphorylation
protein dephosphorylation
peptidyl-tyrosine phosphorylation
regulation of translational elongation
regulation of protein serine/threonine phosphatase activity
small GTPase mediated signal transduction
signal transduction by protein phosphorylation
serine family amino acid metabolic process
fatty acid biosynthetic process
microtubule-based process
transmembrane transport
gluconeogenesis
reductive tricarboxylic acid cycle
trehalose biosynthetic process
carbohydrate transport
water transport
cellulose biosynthetic process
malate metabolic process
starch metabolic process
glycerol transport
endocytosis
glycolytic process
proline metabolic process
aspartate metabolic process
carbohydrate transmembrane transport
cation transmembrane transport
glycerolipid metabolic process
regulation of anion transmembrane transport
multicellular organism development
photomorphogenesis
transmembrane receptor protein serine/threonine kinase signaling pathway
ribosome biogenesis
cellular water homeostasis
lateral root formation
xylem development
abscisic acid-activated signaling pathway
response to ethylene
cell redox homeostasis
cytokinin biosynthetic process
carbon utilization
Genes exlcusively duplicated in C.pepo
NAD biosynthetic process
aerobic respiration
SCF-dependent proteasomal ubiquitin-dependent protein catabolic process
'de novo' AMP biosynthetic process
arginine catabolic process
aspartyl-tRNA aminoacylation
N-terminal protein amino acid acetylation
protein methylation
transcription elongation from RNA polymerase II promoter
protein dephosphorylation
protein-chromophore linkage
DNA-templated transcription, initiation
phosphatidylinositol dephosphorylation
protein ubiquitination
RNA splicing
sialylation
flavonol biosynthetic process
histidine biosynthetic process
sterol biosynthetic process
dolichol metabolic process
glutaminyl-tRNAGln biosynthesis via transamidation
protein N-linked glycosylation via asparagine
lysine biosynthetic process via diaminopimelate
mRNA splicing, via spliceosome
pyridoxine metabolic process
dephosphorylation of RNA polymerase II C-terminal domain
IMP metabolic process
succinate metabolic process
[2Fe-2S] cluster assembly
arginyl-tRNA aminoacylation
cell wall mannoprotein biosynthetic process
D-amino acid catabolic process
glutathione biosynthetic process
cobalamin biosynthetic process
fumarate metabolic process
glucosylceramide biosynthetic process
heme O biosynthetic process
heme oxidation
histone H4-K5 acetylation
keratan sulfate biosynthetic process
strigolactone biosynthetic process
leucyl-tRNA aminoacylation
L-proline biosynthetic process
photoreactive repair
polyamine catabolic process
protein arginylation
multidimensional cell growth
cytidine deamination
maintenance of DNA methylation
putrescine biosynthetic process from arginine
regulation of DNA methylation
regulation of inositol trisphosphate biosynthetic process
SREBP signaling pathway
mitochondrial electron transport, NADH to ubiquinone
xylulose metabolic process
'de novo' pyrimidine nucleobase biosynthetic process
dTMP biosynthetic process
polynucleotide 5' dephosphorylation
protein delipidation
succinyl-CoA metabolic process
tRNA 5'-leader removal
urate catabolic process
ubiquinone biosynthetic process
lipid catabolic process
photorespiration
ent-kaurene oxidation to kaurenoic acid
non-photoreactive DNA repair
protein ufmylation
thiazole biosynthetic process
nucleoside triphosphate biosynthetic process
lipid metabolic process
protein O-linked mannosylation
DNA replication initiation
glucuronoxylan biosynthetic process
fructose 2,6-bisphosphate metabolic process
nucleotide-excision repair involved in interstrand cross-link repair
transcription-coupled nucleotide-excision repair
regulation of dephosphorylation
carbohydrate catabolic process
mitochondrial respiratory chain complex IV assembly
regulation of mitotic spindle organization
rRNA modification
Golgi organization
regulation of signal transduction
systemic acquired resistance, salicylic acid mediated signaling pathway
positive regulation of gibberellic acid mediated signaling pathway
formation of translation preinitiation complex
methylation-dependent chromatin silencing
positive regulation of G2/M transition of mitotic cell cycle
regulation of ruffle assembly
retrograde transport, vesicle recycling within Golgi
response to desiccation
defense response to insect
response to low fluence blue light stimulus by blue low-fluence system
response to bacterium
vesicle fusion
production of ta-siRNAs involved in RNA interference
vesicle docking
chromatin organization
actin filament reorganization
response to carbon dioxide
activation of phospholipase C activity
cellular response to carbon dioxide
chromatin remodeling
barrier septum site selection
negative regulation of translational elongation
positive regulation by host of viral process
regulation of gene expression
positive regulation of catalase activity
regulation of carbon utilization
nuclear pore organization
cytoplasmic translational termination
regulation of asymmetric cell division
regulation of phragmoplast microtubule organization
chloroplast-nucleus signaling pathway
negative regulation of cytokinin dehydrogenase activity
regulation of endoplasmic reticulum unfolded protein response
response to nematode
regulation of cell cycle
intracellular distribution of mitochondria
regulation of methylation-dependent chromatin silencing
viral gene silencing in virus induced gene silencing
regulation of stomatal opening
negative regulation of ER-associated ubiquitin-dependent protein catabolic process
response to benzoic acid
UV protection
intracellular protein transport
chloroplast accumulation movement
NLS-bearing protein import into nucleus
protein export from nucleus
pollen development
phloem development
vegetative phase change
photosynthesis, light harvesting in photosystem I
protein import into peroxisome matrix
alpha-ketoglutarate transport
attachment of peroxisome to chloroplast
meristem structural organization
regulation of development, heterochronic
cuticle hydrocarbon biosynthetic process
photosynthetic NADP+ reduction
sodium ion transport
choline transport
phosphate ion transmembrane transport
polysaccharide transport
embryo development ending in seed dormancy
anatomical structure morphogenesis
multicellular organismal water homeostasis
protein folding
establishment of spindle pole body localization to nuclear envelope
protein retention in Golgi apparatus
sieve element differentiation
mRNA transport
ATP hydrolysis coupled proton transport
oxaloacetate(2-) transmembrane transport
transport of virus in host, tissue to tissue
vesicle-mediated transport
regulation of adaxial/abaxial pattern formation
trichoblast differentiation
methylation
secondary shoot formation
photosynthesis
reactive oxygen species metabolism

Supplementary Table 1. Accessions of domesticated and wild *Cucurbita* spp. used for transcriptomic and phylogenetic analyses. Number of reads used for assembly the transcriptomes, and number of genes and transcripts obtained are also shown.

Code	Donor bank	Species	Subspecies (cultivar-group)	Country	Observations*	Number of reads	Number of genes	Number of transcripts
BGV004370	COMAV	*C. pepo*	*pepo* (Zucchini)	Spain		1,892,580	18,446	18,902
BGV005382	COMAV	*C. pepo*	*ovifera* (Scallop)	Spain		3,858,970	30,202	31,603
PI 615111	USDA	*C. pepo*	*ovifera* (Acorn)	USA		7,305,712	43,585	47,003
CATIE 18887	CATIE	*C. pepo*	*pepo* (Pumpkin)	Mexico		9,043,764	48,101	52,134
CATIE 11368	CATIE	*C. pepo*	*pepo* (Pumpkin)	Guatemala		7,881,248	44,956	48,891
PI 532354	USDA	*C. pepo*	*fraterna*	Mexico		14,574,156	54,631	63,051
PI 614701	USDA	*C. pepo*	*ozarkana*	USA	Reclassified as fraterna based on fruit traits	11,131,674	41,507	45,626
Nigerian Local	Seed company	*C. moschata*		Nigeria		11,013,414	46,834	51,731
PI 498429	USDA	*C. moschata*		Colombia		6,371,004	47,871	52,874
PI 653064	USDA	*C. moschata*		Nigeria		8,793,992	40,308	43,531
BGV004558	COMAV	*C. maxima*		Argentina		7,687,590	49,103	55,178
VIR 3202	VIR	*C. maxima*		Chile		6,941,722	45,663	49,882
UPV035142	COMAV	*C. maxima*		Angola		8,444,322	51,958	59,291
PI 458653	USDA	*C. maxima*	*andreana*	Argentina		9,186,758	39,317	42,617
PI 512115	USDA	*C. argyrosperma*	*argyrosperma*	Guatemala		8,431,320	44,179	50,119
PI 451712	USDA	*C. argyrosperma*	*argyrosperma*	USA		17,537,688	56,350	69,160
PI 438547	USDA	*C. argyrosperma*		Belize		13,654,318	50,299	58,029
PI 202079	USDA	*C. argyrosperma*	*argyrosperma*	Mexico		10,173,060	43,676	48,547
PI 512114	USDA	*C. argyrosperma*	*argyrosperma*	Nicaragua		8,312,838	37,028	40,099
CATIE 16038	CATIE	*C. ficifolia*		Guatemala		11,304,986	40,213	43,269
CATIE 16575	CATIE	*C. ficifolia*		Guatemala		11,415,514	54,537	60,549

PI 432441	USDA	*C. ecuadorensis*		Ecuador		7,045,030	39,920	42,730
PI 432443	USDA	*C. ecuadorensis*		Ecuador		5,165,038	43,184	46,323
Grif 9446	USDA	*C. ecuadorensis*		Ecuador		11,424,844	49,330	54,999
PI 532363	USDA	*C. okeechobeensis*	*martinezii*	Mexico		9,208,076	39,684	42,810
PI 512105	USDA	*C. okeechobeensis*	*martinezii*	Mexico		5,670,572	42,321	45,035
PI 512106	USDA	*C. okeechobeensis*	*martinezii*	Mexico		4,097,656	42,418	45,173
PI 438542	USDA	*C. lundelliana*		Belize		10,515,350	45,096	49,266
PI 532357	USDA	*C. lundelliana*		Mexico		6,957,802	40,933	44,365
PI 636138	USDA	*C. lundelliana*		Belize		11,478,416	52,299	57,111
PI 540898	USDA	*C. lundelliana*		Honduras		7,510,758	53,599	59,801
PI 442197	USDA	*C. foetidissima*		Mexico		7,893,284	50,770	58,496
PI 532350	USDA	*C. foetidissima*		Mexico		8,023,710	39,222	44,100
PI 442201	USDA	*C. foetidissima*		Mexico	Possible hybrid based on morphology	12,257,620	54,205	65,217
PI 532392	USDA	*C.* x *scabridifolia*		Mexico	Hybrid C. foetidissima x C. scabridifolia	9,427,190	42,885	48,184
PI 653839	USDA	*C. cordata*		Mexico		5,055,088	38,784	41,705
Grif 9445	Seed company	*C. cordata*		Mexico		5,756,634	33,530	36,153
PI 442341	USDA	*C. pedatifolia*		Mexico		8,712,776	39,572	45,615
PI 442290	USDA	*C. pedatifolia*		Mexico		27,822,108	67,366	92,522
PI 540737	USDA	*C. pedatifolia*		Mexico	Hybrid C. pedatifolia x C. foetidissima	7,485,656	35,562	39,306

* These accessions were morphologically characterized to confirm their taxonomic classification. Some of them were proved to be misclassified.

Supplementary Table 2. NGS library statistics. Numbers of raw reads, percentage of nucleotides over a 30 quality, coverage, % of reads filtered out during the cleaning process, % of reads without adaptor, % of chimeric reads, number of cleaned reads, coverage of cleaned reads, and percentage of nucleotides over a 30 quality in the clean reads.

Library	**# Raw reads**	**Q30**	**Coverage**	**% Cleaned**	**% Category D**	**% Chimeric**	**# Filtered reads**	**Coverage clean**	**% Q30 clean**
Pair-end	882,803,080	88.60	254	43.00	--	--	503,219,464	145	99.98
3 Kb	186,878,960	91.32	54	49.60	--	24.53	71,085,422	31	99.96
7 Kb	159,602,336	90.74	46	73.67	--	26.94	30,700,824	13	99.94
10 Kb	149,980,526	89.62	65	48.40	28.59	3.55	53,381,028	23	99.986
20 Kb	143,080,152	88.14	62	69.22	30.12	4.75	30,047,048	13	99.82

Supplementary Table 3. Scaffolds of genome assembly v.3.2. containing chloroplastic and mitochondrial regions. The pseudochromosomes were build out of the version 3.2 scaffolds

Mitochondrion			**Chloroplast**
CP32_scaffold000204	CP32_scaffold000212	CP32_scaffold000255	CP32_scaffold000227
CP32_scaffold000205	CP32_scaffold000213	CP32_scaffold000256	CP32_scaffold000415
CP32_scaffold000206	CP32_scaffold000214	CP32_scaffold000257	CP32_scaffold000421
CP32_scaffold000207	CP32_scaffold000215	CP32_scaffold000258	CP32_scaffold000922
CP32_scaffold000208	CP32_scaffold000216	CP32_scaffold000259	CP32_scaffold001585
CP32_scaffold000209	CP32_scaffold000217	CP32_scaffold000260	CP32_scaffold002404
CP32_scaffold000210	CP32_scaffold000218	CP32_scaffold000261	CP32_scaffold002426
CP32_scaffold000211	CP32_scaffold000219	CP32_scaffold000262	CP32_scaffold002979
CP32_scaffold000212	CP32_scaffold000220	CP32_scaffold000263	CP32_scaffold003103
CP32_scaffold000213	CP32_scaffold000221	CP32_scaffold000264	CP32_scaffold003469
CP32_scaffold000214	CP32_scaffold000222	CP32_scaffold000265	CP32_scaffold003889
CP32_scaffold000215	CP32_scaffold000223	CP32_scaffold000266	CP32_scaffold005778
CP32_scaffold000216	CP32_scaffold000224	CP32_scaffold000267	CP32_scaffold007510
CP32_scaffold000217	CP32_scaffold000225	CP32_scaffold000268	
CP32_scaffold000218	CP32_scaffold000226	CP32_scaffold000269	
CP32_scaffold000219	CP32_scaffold000227	CP32_scaffold000270	
CP32_scaffold000220	CP32_scaffold000228	CP32_scaffold000271	
CP32_scaffold000221	CP32_scaffold000229	CP32_scaffold000272	
CP32_scaffold000222	CP32_scaffold000230	CP32_scaffold000273	
CP32_scaffold000223	CP32_scaffold000231	CP32_scaffold000274	
CP32_scaffold000224	CP32_scaffold000232	CP32_scaffold000275	
CP32_scaffold000225	CP32_scaffold000233	CP32_scaffold000276	
CP32_scaffold000226	CP32_scaffold000234	CP32_scaffold000277	
CP32_scaffold000227	CP32_scaffold000235	CP32_scaffold000278	

CP32_scaffold000228	CP32_scaffold000236	CP32_scaffold000279
CP32_scaffold000229	CP32_scaffold000237	CP32_scaffold000280
CP32_scaffold000230	CP32_scaffold000238	CP32_scaffold000281
CP32_scaffold000231	CP32_scaffold000239	CP32_scaffold000282
CP32_scaffold000232	CP32_scaffold000240	CP32_scaffold000283
CP32_scaffold000233	CP32_scaffold000241	CP32_scaffold000284
CP32_scaffold000234	CP32_scaffold000242	CP32_scaffold000285
CP32_scaffold000235	CP32_scaffold000243	CP32_scaffold000286
CP32_scaffold000236	CP32_scaffold000244	CP32_scaffold000287
CP32_scaffold000237	CP32_scaffold000245	CP32_scaffold000288
CP32_scaffold000238	CP32_scaffold000246	CP32_scaffold000289
CP32_scaffold000239	CP32_scaffold000247	CP32_scaffold000290
CP32_scaffold000240	CP32_scaffold000248	CP32_scaffold000291
CP32_scaffold000241	CP32_scaffold000249	CP32_scaffold000292
CP32_scaffold000242	CP32_scaffold000250	CP32_scaffold000293
CP32_scaffold000243	CP32_scaffold000251	CP32_scaffold000294
CP32_scaffold000244	CP32_scaffold000252	CP32_scaffold000295
CP32_scaffold000245		

Supplementary Table 4. Genome v.4.1 pseudochromosomes configuration. The order, orientation and size of genome v. 3.2 scaffolds grouped in each pseudochromosomes is shown. Equivalence of pseudochromosomes and linkage groups of Montero-Pau et al. (2016) genetic map is also shown.

Genome v.4.1 pseudochromosome	**Genetic map linkage group in Montero-Pau et al. 2016**	**Scaffold order**	**Scaffold name**	**Scaffold size**	**Scaffold orientation**
CP4.1LG01	LG01	1	CP32_scaffold000010	3,883,160	reverse
		2	CP32_scaffold000175	233,039	reverse
		3	CP32_scaffold000046	1,602,464	reverse
		4	CP32_scaffold000051	1,450,516	reverse
		5	CP32_scaffold000040	1,852,384	reverse
		6	CP32_scaffold000144	331,714	forward
		7	CP32_scaffold000084	741,359	forward
		8	CP32_scaffold000063	1,087,272	forward
		9	CP32_scaffold000111	460,681	forward
		10	CP32_scaffold000233	109,860	reverse
		11	CP32_scaffold000078	832,487	forward
		12	CP32_scaffold000181	222,517	reverse
		13	CP32_scaffold000059	1,137,078	reverse
		14	CP32_scaffold000079	790,494	forward
		15	CP32_scaffold000087	658,871	reverse
		16	CP32_scaffold000105	507,762	forward
		17	CP32_scaffold000032	2,241,395	forward
		18	CP32_scaffold000024	2,525,860	reverse
		19	CP32_scaffold000091	633,856	forward
CP4.1LG02	LG02	1	CP32_scaffold000001	6,123,784	reverse
		2	CP32_scaffold000128	403,365	reverse
		3	CP32_scaffold000099	554,539	forward

		4	CP32_scaffold000166	257,955	forward
		5	CP32_scaffold000090	642,088	undefined
		6	CP32_scaffold000076	841,349	undefined
		7	CP32_scaffold000055	1,317,493	reverse
		8	CP32_scaffold000162	279,451	reverse
		9	CP32_scaffold000208	154,271	forward
		10	CP32_scaffold000374	40,295	undefined
		11	CP32_scaffold000140	338,305	forward
		12	CP32_scaffold000062	1,102,807	reverse
		13	CP32_scaffold002675	2,094	undefined
		14	CP32_scaffold000169	245,895	reverse
		15	CP32_scaffold000041	1,808,812	reverse
		16	CP32_scaffold000168	248,911	forward
CP4.1LG03	LG03	1	CP32_scaffold000038	1,877,481	reverse
		2	CP32_scaffold000122	422,066	reverse
		3	CP32_scaffold000195	188,662	forward
		4	CP32_scaffold000019	3,089,961	reverse
		5	CP32_scaffold000117	430,983	reverse
		6	CP32_scaffold000210	151,564	forward
		7	CP32_scaffold000163	278,935	forward
		8	CP32_scaffold000177	230,436	undefined
		9	CP32_scaffold000118	428,730	forward
		10	CP32_scaffold000187	210,711	forward
		11	CP32_scaffold000006	4,754,185	reverse
		12	CP32_scaffold000044	1,697,700	reverse
CP4.1LG04	LG18 + LG20	1	CP32_scaffold000027	2,403,537	reverse
		2	CP32_scaffold000207	155,442	forward
		3	CP32_scaffold000002	5,399,389	reverse
		4	CP32_scaffold000025	2,522,528	reverse

		5	CP32_scaffold000033	2,224,244	forward
CP4.1LG05	LG04	1	CP32_scaffold000066	995,157	reverse
		2	CP32_scaffold000180	223,211	reverse
		3	CP32_scaffold000143	334,696	forward
		4	CP32_scaffold000086	693,282	reverse
		5	CP32_scaffold000159	289,565	forward
		6	CP32_scaffold000022	2,747,443	forward
		7	CP32_scaffold000021	2,780,951	forward
		8	CP32_scaffold000020	2,794,373	forward
CP4.1LG06	LG07	1	CP32_scaffold000035	2,140,805	forward
		2	CP32_scaffold000083	758,721	reverse
		3	CP32_scaffold000042	1,749,822	forward
		4	CP32_scaffold000043	1,732,427	reverse
		5	CP32_scaffold000082	760,949	reverse
		6	CP32_scaffold000185	216,892	forward
		7	CP32_scaffold013127	333	forward
		8	CP32_scaffold000158	289,633	reverse
		9	CP32_scaffold000036	2,105,938	reverse
		10	CP32_scaffold000106	503,388	forward
		11	CP32_scaffold000127	408,837	forward
CP4.1LG07	LG15	1	CP32_scaffold000060	1,133,474	forward
		2	CP32_scaffold000093	615,043	reverse
		3	CP32_scaffold000056	1,254,317	forward
		4	CP32_scaffold000097	558,874	reverse
		5	CP32_scaffold000069	945,996	reverse
		6	CP32_scaffold000135	366,381	reverse
		7	CP32_scaffold000119	428,542	reverse
		8	CP32_scaffold000133	378,800	undefined
		9	CP32_scaffold000023	2,545,012	forward

		10	CP32_scaffold000138	352,159	reverse
		11	CP32_scaffold000214	135,984	forward
		12	CP32_scaffold000172	241,243	reverse
		13	CP32_scaffold000092	623,336	forward
		14	CP32_scaffold000098	555,395	reverse
CP4.1LG08	LG06	1	CP32_scaffold000003	4,875,806	reverse
		2	CP32_scaffold000089	642,205	forward
		3	CP32_scaffold000008	3,995,464	forward
		4	CP32_scaffold000101	542,828	forward
CP4.1LG09	LG08	1	CP32_scaffold000014	3,564,952	forward
		2	CP32_scaffold000251	101,034	forward
		3	CP32_scaffold000061	1,116,870	reverse
		4	CP32_scaffold000132	379,208	reverse
		5	CP32_scaffold000245	101,953	forward
		6	CP32_scaffold000247	101,524	reverse
		7	CP32_scaffold000145	331,494	undefined
		8	CP32_scaffold000075	863,406	forward
		9	CP32_scaffold000072	896,126	forward
		10	CP32_scaffold000026	2,454,755	forward
CP4.1LG10	LG10	1	CP32_scaffold000009	3,958,430	reverse
		2	CP32_scaffold000029	2,358,218	reverse
		3	CP32_scaffold000068	950,888	reverse
		4	CP32_scaffold000125	410,804	forward
		5	CP32_scaffold000160	285,501	forward
		6	CP32_scaffold000057	1,171,448	reverse
		7	CP32_scaffold000171	242,204	reverse
		8	CP32_scaffold000114	450,599	reverse
CP4.1LG11	LG13	1	CP32_scaffold000107	498,007	reverse
		2	CP32_scaffold000017	3,213,514	forward

		3	CP32_scaffold000108	488,883	forward
		4	CP32_scaffold000124	411,803	reverse
		5	CP32_scaffold000141	338,006	forward
		6	CP32_scaffold000088	647,301	reverse
		7	CP32_scaffold000113	452,942	reverse
		8	CP32_scaffold000049	1,492,573	forward
		9	CP32_scaffold000053	1,373,939	forward
		10	CP32_scaffold000094	602,087	forward
		11	CP32_scaffold000153	304,914	forward
CP4.1LG12	LG05	1	CP32_scaffold000012	3,815,302	forward
		2	CP32_scaffold000121	422,947	reverse
		3	CP32_scaffold000071	899,720	forward
		4	CP32_scaffold000018	3,164,343	reverse
		5	CP32_scaffold000048	1,517,882	reverse
CP4.1LG13	LG16	1	CP32_scaffold000085	695,292	forward
		2	CP32_scaffold000034	2,168,721	forward
		3	CP32_scaffold000129	385,840	forward
		4	CP32_scaffold000225	119,458	reverse
		5	CP32_scaffold000080	770,750	forward
		6	CP32_scaffold000028	2,396,146	reverse
		7	CP32_scaffold000030	2,292,851	reverse
		8	CP32_scaffold000104	518,031	forward
CP4.1LG14	LG19	1	CP32_scaffold000005	4,849,021	reverse
		2	CP32_scaffold000147	327,288	undefined
		3	CP32_scaffold000182	222,078	undefined
		4	CP32_scaffold000050	1,454,989	forward
		5	CP32_scaffold000037	2,098,557	forward
CP4.1LG15	LG11	1	CP32_scaffold000015	3,441,236	forward
		2	CP32_scaffold000131	379,828	forward

		3	CP32_scaffold000047	1,558,130	forward
		4	CP32_scaffold000016	3,434,250	forward
CP4.1LG16	LG17	1	CP32_scaffold000067	991,265	reverse
		2	CP32_scaffold000200	168,863	forward
		3	CP32_scaffold000164	278,388	undefined
		4	CP32_scaffold000256	97,354	undefined
		5	CP32_scaffold000070	928,547	forward
		6	CP32_scaffold000206	156,815	undefined
		7	CP32_scaffold000152	310,330	forward
		8	CP32_scaffold000100	550,348	forward
		9	CP32_scaffold000142	337,580	forward
		10	CP32_scaffold000004	4,863,444	forward
CP4.1LG17	LG12	1	CP32_scaffold000103	531,021	reverse
		2	CP32_scaffold000065	997,141	forward
		3	CP32_scaffold000074	869,430	reverse
		4	CP32_scaffold000096	589,541	forward
		5	CP32_scaffold000120	423,438	reverse
		6	CP32_scaffold000186	215,517	forward
		7	CP32_scaffold000058	1,167,845	forward
		8	CP32_scaffold000031	2,250,994	reverse
		9	CP32_scaffold000045	1,627,577	forward
CP4.1LG18	LG14	1	CP32_scaffold000073	884,058	forward
		2	CP32_scaffold000095	591,145	forward
		3	CP32_scaffold000116	432,341	forward
		4	CP32_scaffold000157	293,129	forward
		5	CP32_scaffold000112	453,344	forward
		6	CP32_scaffold000039	1,853,076	forward
		7	CP32_scaffold000011	3,820,361	forward
CP4.1LG19	LG09	1	CP32_scaffold000054	1,345,344	forward

		2	CP32_scaffold000064	1,081,996	forward
		3	CP32_scaffold000161	281,296	forward
		4	CP32_scaffold000197	183,073	reverse
		5	CP32_scaffold000146	330,575	forward
		6	CP32_scaffold000077	836,762	reverse
		7	CP32_scaffold000130	382,378	reverse
		8	CP32_scaffold000013	3,798,258	reverse
CP4.1LG20	LG21	1	CP32_scaffold000007	4,346,540	forward
		2	CP32_scaffold000148	327,036	reverse
		3	CP32_scaffold000115	449,779	forward
		4	CP32_scaffold000110	469,294	forward
		5	CP32_scaffold000151	313,452	forward
		6	CP32_scaffold000081	769,043	reverse
		7	CP32_scaffold000052	1,439,660	reverse

Supplementary Table 5. Summary of repetitive elements found in *Cucurbita pepo, Cucumis melo, Cucumis sativus* and *Citrullus lanatus.* All results are expressed in bp.

Size (bp)	***Cucurbita pepo***	***Cucumis melo***	***Citrullus lanatus***	***Cucumis sativus*** **Chinese long**	***Cucumis sativus*** **PI183967**
Genome size	289504453	406928820	355247419	197271687	204803225
Genome size without Ns	247816929	336097957	321405453	193700889	200988521
Repetitive	93650597	190225685	186381889	55566601	63676019
Repetitive (no overlapping)	85581680	179982107	173126881	52923711	60250642
over_same	4361793	5007047	5992548	1199958	1697636
over_diff	3707124	5236531	7262460	1442932	1727741
DNA		193677	283426	54557	
DNA/CMC-EnSpm	88523	11363266	2589519	1551581	1955210
DNA/Crypton-C			7193		
DNA/En-Spm			139908		
DNA/Ginger			121896	134666	
DNA/IS3EU					82374
DNA/Kolobok-T2	27949				58226

DNA/MULE-MuDR	145882	4697101	1633726	1195740	1003127
DNA/Maverick			192173		
DNA/MuDR		929167	122428	136004	148317
DNA/MuLE-MuDR		6548932	4029767	890154	996088
DNA/PIF-Harbinger	12213	3090436	1290961	550468	343060
DNA/TcMar-Mariner			3360		
DNA/Zisupton				25310	
DNA/hAT-Ac	1246686	728666	1709109	264199	479104
DNA/hAT-Charlie		148193	38283	60790	
DNA/hAT-Tag1	159459	383200	478025	345958	361065
DNA/hAT-Tip100		379594	83286	367630	83315
DNA/hAT-hATm			2825369		
LINE/CR1				36758	21279
LINE/CRE	169102		31891	20041	
LINE/I-Jockey		301			
LINE/L1	2207438	5388043	5944566	2957971	3237632
LINE/L1-DRE			217246		86388

LINE/L1-Tx1	194920	201316	224728	23383	
LINE/L2		24417	950717	70984	
LINE/RTE-BovB	143		185123		104075
LINE/Tad1	68219				117729
LTR	65446	200156	263981	334749	
LTR/Cassandra	1310467	387478	346831	236843	41046
LTR/Caulimovirus	719038	1100094	225529	122829	55250
LTR/Copia	6667202	39238863	33496488	9503582	10759234
LTR/DIRS	150502				
LTR/ERV1		189116			12581
LTR/ERVK	30609				
LTR/ERVL			136788		
LTR/Gypsy	8160792	43716718	31453573	5844651	7988269
LTR/Pao		12326			32675
RC/Helitron	181502	632496	114736	71766	48395
Retroposon				73613	
SINE/Alu					48743

SINE/B2	11862		11186		
SINE/ID	175670				
SINE/tRNA	200088	333231	686539	255170	246352
SINE/tRNA-R2	23160				
SINE/tRNA-RTE	76347				
SINE?	1376290	2458	20168		41669
Satellite	399460	232131		13933	6340
Satellite/Y-chromosome	31503				
Satellite/centr					63047
Simple repeats	8092785	5360259	5874319	3676307	4190723
Low complexity regions	1229916	1395906	1646367	1175901	1160849
rRNA	468015	176725	41472	50262	109384
snRNA	29907	7471	6485	6750	4777
Unknown/undefined	59929502	63163948	88954727	25514051	29789696

Supplementary Table 6. Gene family (orthogroups and paralogs in OrthoMCL) identification.

Species	**# proteins**	**# assigned to a gene family (several species)**	**% assigned**	**# assigned to a gene family (species exclusive)**	**% assigned to a gene family (species exclusive)**	**% of proteins assigned**
Cucurbita pepo	27,870	25,433	91.23	291	1.04	95.26
Citrullus lanatus	23,440	18,798	80.20	2,601	11.10	94.16
Cucumis melo	27,427	19,974	72.83	3,570	13.02	88.22
Cucumis sativus Chinese Long	23,248	19,111	82.20	394	1.69	86.94
Cucumis sativus PI183967	22,790	19,360	84.95	370	1.62	89.48